Rules of Contact Inhibition of Locomotion for Cell-pairs Migrating on Aligned and Suspended Nanofibers

Jugroop Singh

Thesis submitted to the faculty of the Virginia Polytechnic Institute and State University in partial fulfillment of the requirements for the degree of

Master of Science

In

Biomedical Engineering

Amrinder S. Nain, Chair

Bahareh Behkam

Rafael V. Davalos

September 30, 2019

Blacksburg, VA

Keywords: Contact inhibition of locomotion, rules, nanofibers, cell collisions, spindle, parallel

Rules of Contact Inhibition of Locomotion for Cell-pairs Migrating on Aligned and Suspended Nanofibers

Jugroop Singh

ABSTRACT

Contact inhibition of locomotion (CIL), a migratory mechanism, first introduced by Abercrombie and Heaysman in 1953 is now a fundamental driving force in developmental, repair and disease biology. Much of what we know of CIL stems from studies done on 2D substrates which are unable to provide the essential biophysical cue of fibrous extracellular matrix curvature. Here we inquired if the same rules are applicable for cells attached to and migrating persistently on suspended and aligned ECM-mimicking nanofibers. Using two elongated cell shapes (spindle attached to one fiber, and parallel attached to two fibers), we quantitate CIL rules for spindle-spindle, parallel-parallel and spindle-parallel collisions. Two approaching spindles do not repolarize upon contact but rather continue to migrate past one another. Contrastingly, approaching parallel cells establish distinct CIL, with only one cell repolarizing upon contact followed by migration of both cells as a cohesive unit in the repolarization direction. Interestingly, for the case of spindle and parallel cell collision, we find the parallel cell to shift the morphology to that of spindle and continue persistent movement without repolarization. To account for effect of cell speed, we also quantitate CIL collisions between daughter and non-dividing cells. While spindle-spindle collisions result in cells still walking by, for parallel-parallel collisions, we capture rare events of a daughter cell pushing the non-dividing cell. With increasing population numbers, we observe formation of cell streams that collapse into spheroids. Single cells are able to invade along fibers from the spheroids and are then subject to same CIL conditions, thus providing a platform with cyclic CIL. The presented coupling of experimental and analytical framework provides new insights in contextually relevant CIL and predictive capabilities in cell migration decision steps.

Rules of Contact Inhibition of Locomotion for Cell-pairs Migrating on Aligned and Suspended Nanofibers

Jugroop Singh

GENERAL AUDIENCE ABSTRACT

Contact inhibition of locomotion (CIL) is a migratory process that can lead to a change in migration direction through protrusion inhibition of single cells. First described in 1953, the traditional model of CIL shows that on a 2D substrate, two migrating cells experience a decrease in protrusive behavior upon contacting each other, followed by repolarization, and migration away from one another. However, a cell's extracellular matrix (ECM) is fibrous in nature, and how cells maintain standard CIL rules in fibrous environments remains unclear. Here, using suspended, aligned nanofibers created using a non-electrospinning Spinneret based Tunable Engineered Parameters (STEP) method, we investigate CIL decision steps of two fibroblast cells approaching each other in two shapes: spindle cells attached to single fibers, and parallel cells attached to two fibers. Most spindle cells approaching each other do not switch direction upon contact, but rather continue to migrate past each other, termed a walk past. Contrastingly, approaching parallel cells display unique CIL whereby only one cell repolarizes and reverses its migration direction. Subsequently, both cells remain in contact while migrating in the repolarization direction. Interestingly, we report that both spindle and parallel CIL are also affected by speed post cell division. Altogether, for the first time, we introduce a platform to understand cell shape driven CIL geometrical rules in ECM mimicking environments.

Acknowledgments

I'd like to start by thanking my advisor, Dr. Nain, for all of his insights and assistance during my time in STEP lab. I really enjoyed our conversations about different research topics and learned a great deal about skills required to succeed personally and professionally moving forward. I'd also like to thank my committee members, Dr. Behkam and Dr. Davalos for their continued willingness to discuss my research and serve on my committee.

I would not have made it this far without the help and support of all the STEP lab members. To Abinash, Aniket, Appy and Alex, thank you for your patience and kindness while teaching me the skills needed for my research projects. I've been able to take away so much more than just knowledge about science and academic goals through my years here with all of you. I want to thank you the most for your friendship and I wish you all the happiness and success in your lives ahead.

Most of all I owe this accomplishment to my family and friends. I want to thank my mom and dad for being my cheerleaders and always encouraging and supporting me through all my years of school. I would not have been able to succeed if it weren't for your unconditional love. To my sister, you've been my rock and biggest support system for my whole life and even though you couldn't always physically be present, you never made me feel your absence. Last but not the least, thank you to all my friends from home and Virginia Tech who've been on this journey with me. You know who you are, and your support and love will never go unnoticed.

I'd like to conclude by thanking everyone apart of the Virginia Tech community; the students, faculty and staff. Thank you for allowing me to call this place home for the past six years. I can confidently say that Blacksburg, VA will always have a piece of my heart.

Table of Contents

List of Figures

Chapter 1. Introduction

1.1 Cell Migration and Extracellular Matrix

Cell migration is an essential component of various physiological processes such as morphogenesis, wound healing, and metastasis[1]. A cell's extracellular matrix (ECM) is responsible for providing appropriate biophysical and biochemical signals to allow for proper tissue development. The ECM is fibrous in nature and is comprised of various proteins such as collagens, elastins, fibronectins and laminins, with collagen being the most prominent and is also responsible for regulating tissue development, adhesion and migration[2]. Cell-ECM interactions are vital in regulation of cell functions, whether that is seen in wound healing with tissue regeneration or modulating cell proliferation during metastasis[3]. Furthermore, cell polarity is essential for regulating cell-cell communication during migration. This includes molecular cues from proteins or electrochemical signals at a cellular level[4]. Signals include ion fluxes, differences in membrane potential, or electric fields which can contribute to initiation of developmental processes such as wound healing[4]. In order to initiate cell migration processes, cytoskeletal components must be coupled to the ECM through adhesion[5]. A cell's initial response to a migration cue is to put out a protrusion, which can differ in configuration with respect to a lamellipodia or filopodia structure, toward the direction of migration[6].The protrusions are stabilized after adhering to the ECM and the adhesions serve as a pathway for continuous cell migration regulated by actin polymerization[6].

1.2 Importance of Contact Inhibition of Locomotion

Particularly, recent studies involving cell migration have highlighted the influence and dynamics of a cell's molecular machinery with regards to cell polarization and protrusion formation[1,7]. Cell interaction with neighboring cells during migration has also been emphasized in *in vitro* as well as *in vivo* studies, further integrating the relevance of the social behavior of cells[8,9]. This concept of

a cell's social behavior first emerged through *in vitro* studies with chick fibroblasts where the cell migration direction was affected by interaction with other cells[10]. To explain this phenomenon, the term 'contact inhibition of locomotion (CIL)' was coined by Abercrombie and Heaysman nearly five decades ago while studying how the behavior of one cell influences another[9,11]. CIL is the process by which a cell halts its original migration direction upon contact with another cell[11]. The respective steps of CIL include, cell-cell contact, protrusion inhibition at the site of contact, cell repolarization with the formation of new protrusions away from the site of contact, and cell migration in the direction of newly formed protrusions[1]. This sequence can however be altered due to the number of colliding cells as well as in a scenario where only one cell repolarizes while the other maintains its' original migration direction[1]. CIL has also been inferred to influence collective cell migration where the repolarization of cells allow them to interact with other migrating cells, thus forming a collective that continues to migrate as a unit[12–14]. Furthermore a loss of CIL has been shown to occur during metastasis allowing malignant mesenchymal cells to invade fibroblast cultures[11,15,16]. There have been several insights into how a CIL response is activated within cells upon contact to execute the repulsive behavior and switch in polarity. The Rho GTPase family of proteins is essential for directional migration control through regulation of cell protrusions[1,14,17]. Specifically, the RhoA GTP is present at the trailing edge of a cell and activates the protein ROCK, which in turn is responsible for focal adhesion and stress fiber regulation. With respect to CIL, RhoA is essential for the protrusion inhibition prior to repolarization (Figure 1.1). At the leading edge of the cell, Rac1 and Cdc42 control actin polymerization and turnover for the lamellipodium and filopodia respectively. Rac1 is necessary for protrusion formation and stabilization during the CIL process. Furthermore, its been shown that microtubule remodeling is vital for the polarity switch observed in CIL through their

dynamic ability of shrinkage and growth[7]. If ROCK activity is inhibited, this leads to microtubules becoming stabilized, thus diminishing the CIL response between colliding cells. These studies reveal the importance of the molecular machinery of a cell during directed migration processes.

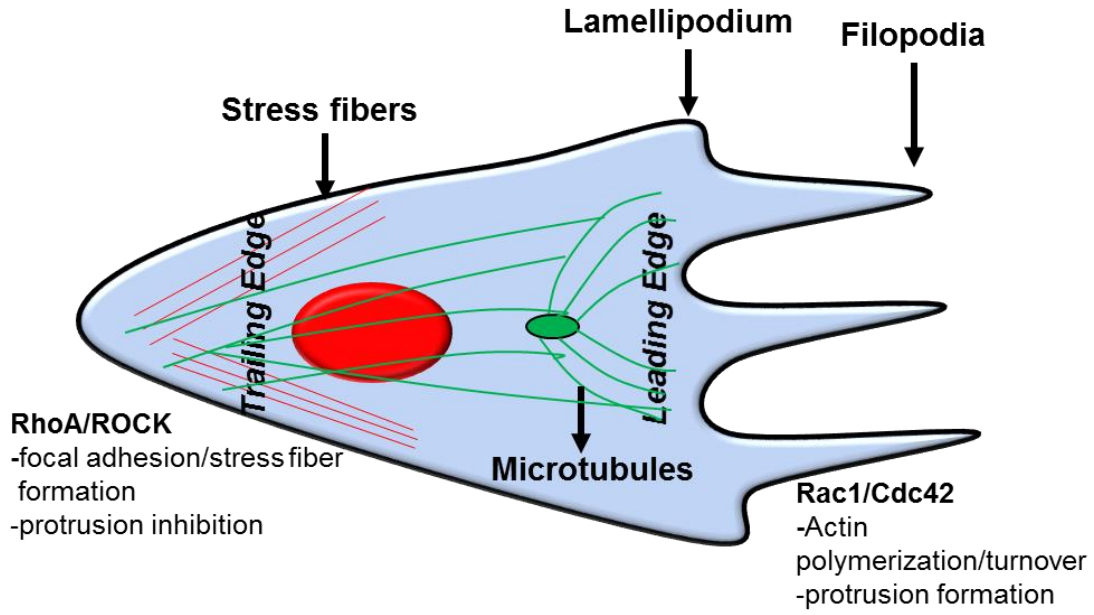

Figure 1.1. Molecular machinery of a cell depicting Rho GTPase control of protrusion behavior.

CIL has implications in several developmental processes necessary to carry out proper cellular function. Studies with *Drosophila* hemocytes show that precise CIL interactions are necessary for proper dispersal. *In vivo* tracking of the actin retrograde flow within hemocytes reveals that synchronized reorganization of the network through adhesion and repulsion is executed, allowing cells to ultimately coordinate their migration[18,19]. This process has been referred to as cellular (neuronal) tiling[19,20]. Additionally, neural crest cells, a migratory, embryonic cellular population requires CIL directed migration *in vitro* and *in vivo* to successfully carry out collective cell migration[1,19,21]. With respect to physiological logical such as wound healing, it has been shown that a loss of heterotypic CIL between leukocytes and fibroblasts, allows the leukocytes to migrate to wound site and repair the injury[19,22]. However, leukocytes still maintain homotypic CIL when

colliding with one another, holding significance in immune activation. Furthermore, a loss of CIL has also been inferred to contribute to disease particularly, metastatic invasion. In his initial studies, Abercrombie implicated the loss of heterotypic CIL between cancer and non-cancerous cell populations[23], however, this does not imply the loss of homotypic CIL as well, which is maintained among cancer cells upon contact.

1.3 Effect of chemical gradients on CIL

CIL has also been studied upon introducing chemical gradients to determine their effect on the outcomes of cell collisions. Specifically, epidermal growth factor (EGF), a well-known attractant related to breast cancer chemotaxis, was incorporated into CIL experiments through utilization of a microfluidic device with 1D microchannels, constraining cell migration. Here, authors showed that EFG-controlled chemotaxis along with CIL affects breast cancer cell migration and an increase of EGF concentration leads to a diminished CIL response[24]. Most frequently for head-head (leading-leading) collisions, authors reported mutual CIL outcomes post contact, wherein both cells from the pair repolarized and altered its migration direction. This was irrespective of the EGF dose. For head-tail (leading-trailing) collisions, authors reported the repulsion and redirection of the trailing cell as the dominant outcome post cell collision.

Additionally, another chemotactic cue reported in CIL studies is stromal cell-derived factor 1 (Sdf-1). With respect to studies conducted with neural crest cells, it has been observed that neural crest cells chemotax toward Sdf-1 which is secreted by placode cells. Upon reaching the placode cells, neural crest cells induce a CIL response which ultimately causes the placode cells to migrate away while neural crest cells follow[25].

1.4 Previous methods to study CIL

CIL is most commonly studied and analyzed on flat curvature lacking 2D substrates utilizing several invasion assay techniques[8,9,26]. As a result, CIL was initially qualitatively and quantitatively recorded based off head-head cell collisions, where the repulsive response can be easily observed. However, 2D assays do not constrain the degree of freedom of randomly migrating cells, which makes quantitating CIL dynamics difficult[26], and recently, micropatterned substrates comprising of fibronectin lines have been utilized to understand restricted motility, such as persistent migration as observed *in vivo*[26–28]. The advantage of these substrates includes the formation of a 1D collision assay where cell migration is constrained to straight lines allowing for a greater occurrence of cell-cell collisions that induce a CIL response. Cells migrating on uniform stiffness assays have near similar speeds and 2D assays define CIL with repolarization of cells, while printed lines intriguingly demonstrate cells sliding past each other as an outcome of cell-cell collisions[26,29] as well as head-tail collisions[14]. Furthermore, based off the extension of CIL studies to 1D collision assays, new definitions of CIL also emerged[19] further adding to the complexity of this process in terms of cell collision outcomes. Generally, CIL has been categorized into two broad subsets, homotypic CIL, referring to collisions between cells of the same type (Figure 1.2a, left) or heterotypic CIL, referring to collisions between two different cell types (Figure 1.2, right) such as cancer cells and fibroblast cells. More specifically, type 1/mutual CIL follows the traditional definition with two cells approaching one another, repolarizing and migrating away post contact (Figure 1.2b). Type II CIL, is defined by two cells approaching and subsequently remaining in contact with one another without repolarization Figure 1.2c). Moreover, non-mutual CIL details two cells approaching, resulting in the repulsion and redirection of a single cell in the pair (Figure 1.2d). Lastly, a loss of CIL is when both approaching cells fail to repolarize and

continue to migrate past each other (Figure 1.2e). These outcomes have expanded due to new experimentation on platforms that can increase the likelihood of single cell collisions

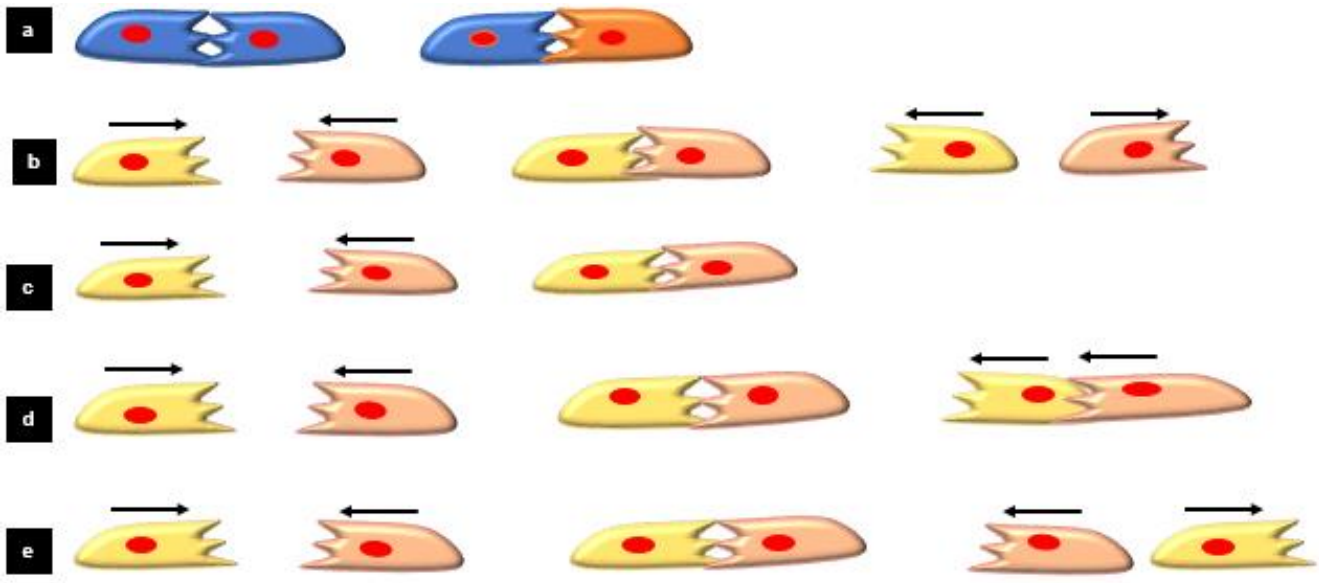

Figure 1.2. Reported CIL outcomes. **a)** Homotypic CIL between two of the same cells (left) and heterotypic between two different cell types (right CIL). **b)** Type 1/mutual CIL. **c)** Type II CIL, showing a cessation of movement. **d)** Non-mutual with repolarization of one cell from the pair. **e)** Loss of CIL with cells migrating past one another without repolarization. Arrows indicate migration direction.

1.5 Step platform and materials and methods

STEP (Spinneret based Tunable Engineered Parameters) is a non-electrospinning technique that has the ability to deposit highly aligned polymeric fibers onto a scaffold with precise control over fiber diameter and spacing[30–34]. The STEP method allows for deposition of fiber diameters ranging from micrometers to as small as 100 nanometers. Additionally, fiber networks of varying architectures can be manufactured to induce diverse cell geometries and morphologies. Furthermore, different polymers can be utilized to manufacture these nanofibers such as polystyrene (PS), polyurethane (PU) and poly(lactic-co-glycolic acid (PGLA) among others. The execution of the STEP platform is accomplished by pulling the chosen polymer solution by the means of mechanical pressure and forming a droplet at the tip of the pipette. The droplet then makes contact with a rotating substrate, termed scaffold, where the breaking of the surface tension allows for fiber deposition onto the scaffold[30]. The advantage of this platform is the fact that it does not require the use of an electric source to manufacture the fibers. Furthermore, the superior fiber alignment and diameter control introduces a platform that mimics an *in vivo* ECM fibrous environment.

1.5.1 Cell Seeding and Imaging

The nanofiber networks were placed in individual wells of a six-well plate and sterilized under UV radiation before coating with 4µg/mL of fibronectin for approximately one hour. 3T3 fibroblasts were cultured in Dulbecco's Modified Eagle Medium (DMEM) supplemented with 10% Fetal Calf Serum (FCS) at 37°C and 5% CO2 in T-25 flasks. The cells were seeded at a low concentration onto the nanofiber networks after removal of the fibronectin and were subsequently left to attach for one hour prior to flooding each well with 3mL of media. Time-lapse imaging for migration

was executed for 24 hours with an imaging interval ranging from 1 minute, 2 minutes or 3 minutes using a 20x objective.

1.5.2 Cell migration analysis

Time-lapse videos were created with spindle and parallel cells prior to contact, during contact, and for some cases post contact. Image J was used to outline cells, track cell centroids and obtain an average migration rate (μm/min) from instantaneous speed calculations every 6 minutes for clean cell collisions pre, during and post contact. Individual spindle and parallel cell migration rate was calculated the same way and an average was obtained and reported per minute. Normalized cell position vs. time transient plots were created by normalizing the cell position from the midpoint of the two cells being analyzed to the starting distance between their centroids. This prevented cells from contacting each other pre-contact and allowed us to track cells post-contact with no contact.

1.5.3 Statistical analysis

Statistical significance was determined using Graphpad Prism software. The D'Agostino and Pearson omnibus normality test was used to test data normality. Following the normality results, either Analysis of Variance, with Tukey's HSD for multiple comparisons or the non-parametric Kruskal-Wallis test, with the Dunn's multiple comparison test was used to specify significance between different groups. For comparisons between two groups, Student t-tests were applied. Standard error was used for error bars (performed in Excel) and significance was reported per standard (****, $p<0.0001$; ***, $p<0.001$; **, $p<0.01$; *, $p < 0.05$).

1.6 Objectives of Study

In vivo, native cellular environments consist of fibrous proteins of varying curvatures deposited in multiple arrangements (dense vs. sparse or isotropic vs. anisotropic) that comprehensively provide a multi-dimensional environment for cells to migrate upon (Figure 1.3).

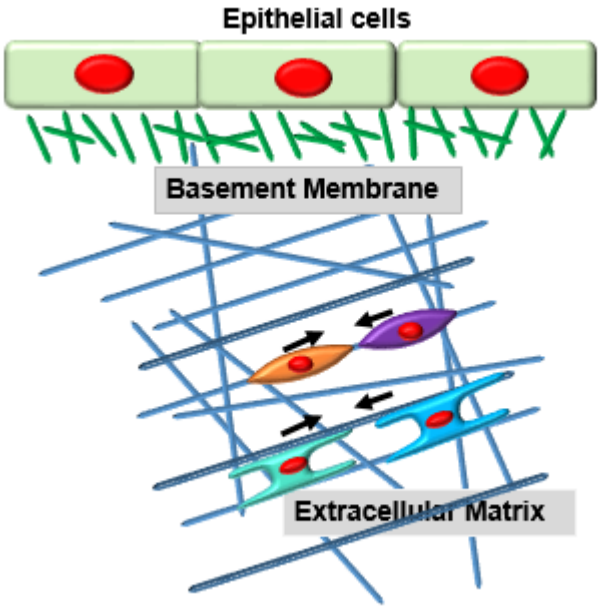

Figure 1.3: Depiction of *in vivo* ECM environment with randomly oriented fibers and cells of spindle and parallel morphologies.

Here, we use our previously described non-electrospinning Spinneret based Tunable Engineered Parameters (STEP) fibrous platform to study CIL[31]. We investigated cell shapes on three varying diameters, small (135nm), intermediate (500nm) and larger (1000nm) and chose to proceed with our CIL studies on the intermediate (500nm) diameter as CIL behavior was more prominent for observation and quantification (Figure 1.4) with respect to protrusion length.

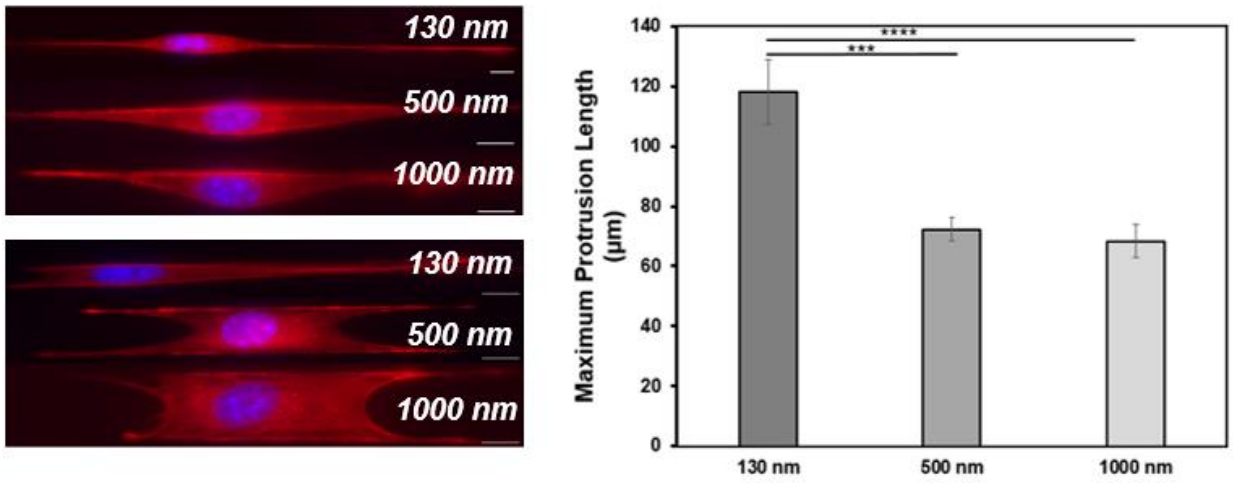

Figure 1.4 Cell shapes on 130nm, 500nm, and 1000nm with comparison of protrusion lengths (n=30 each). Cells are stained for actin (red) and the nucleus (blue). (****, $p<0.0001$; ***, $p<0.001$). Scale bars: 10µm

We manufacture aligned nanofiber networks to study CIL behavior in NIH/3T3 fibroblast cell-cell pairs exhibiting two distinct elongated morphologies, spindle, attached to a single fiber and parallel, attached to two fibers[34] (Figure 1.5). We further investigate the role of cell speed on CIL by incorporating CIL between faster mitotic daughters and slower moving fibroblasts. We design our fiber networks to mimic sparse fibrous environments that promote attachment and migration of single cells[35–37]. Studying cells in two common shapes but different focal adhesion patterns (two focal adhesion clusters in spindle vs. four in parallel) allows for an expanded understanding of contact inhibition geometric rules. In accordance with CIL behavior reported on micropatterned lines, we observe that upon contact most spindle cells walk past one another without a change in direction. In contrast, cells with a parallel morphology most commonly undergo non-mutual CIL where they maintain contact with an inability to cross over one another, which leads to repolarization of a single cell. Following cell division, spindle cells have higher number of cells exhibiting slide-by behavior, while interestingly, parallel shaped, fast moving daughter cells induce two new modes: cells slide-by each other by assuming a spindle shape, and remarkable ability to ‘jam’ and subsequently ‘push’ another parallel cell, leading to cell repolarization in the

opposite direction of migration. Independent of cell shape, with increasing number of cells, we report a general loss of CIL that promotes formation of multi-cellular chains. On occasion, chains can collapse to form cellular spheroids of varying sizes, from which invasion of cells is resumed followed by subjection to CIL rules described above, thus completing the cycle of cellular aggregation and dissemination. *In vitro* recapitulation of curvature effects by us previously has shown both protrusive and migratory sensitivity to fibers of varying diameters. Furthermore, we have shown that suspended flat 2D ribbons do not capture the protrusive behavior observed on suspended round fibers, thus, we wanted to inquire if the generally understood CIL rules developed on 2D assays extended to contextually relevant fibrous environments.

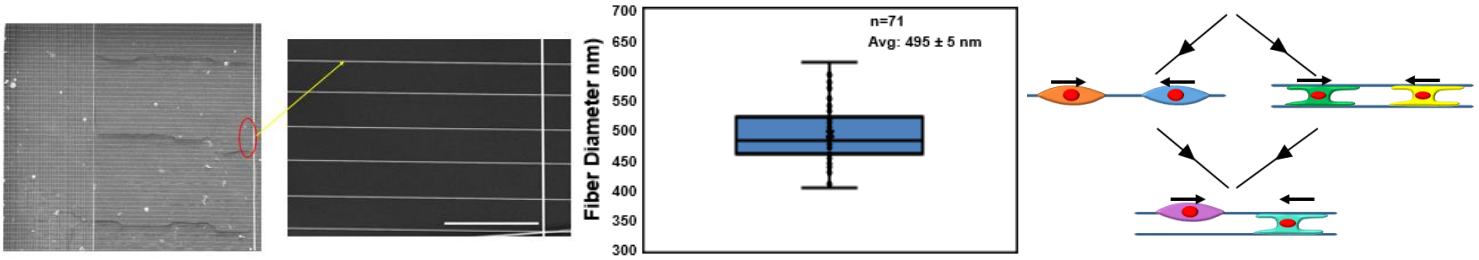

Figure 1.5: STEP fiber network. Parallel migration scaffolds with aligned geometries and 500nm diameter used to study CIL (box plot) in spindle and parallel shaped cells. Scale bar: 50µm.

Chapter 2. Spindle cell CIL

2.1 Leading-Leading collisions without cell division

We looked at 50 independent and randomly selected approaching spindle cell-cell interactions without division from 40 experiments. We found that 67% of collisions involved two cells approaching each other and walking past one other without repolarizing (Figure 2.1).

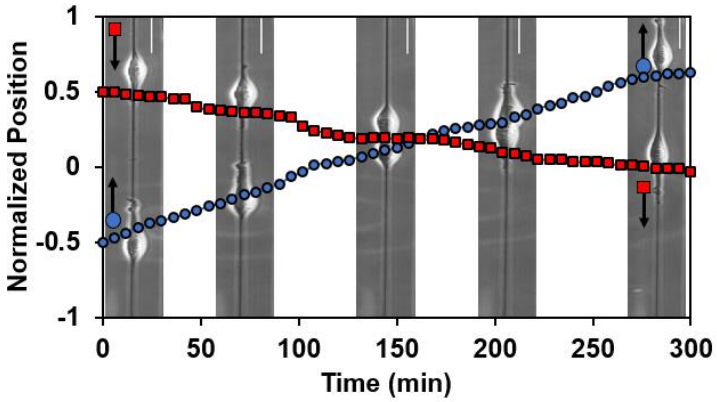

Figure 2.1. Transient profile of two approaching spindles walking past one another without repolarization. Scale bars: 50µm

We then quantified the speeds of 18 of these collisions looking at periods of pre contact, during contact and post contact and found that cells experienced a reduction in speed during the contact period and regained speed post contact without a statistical change in speed (Figure 2.2).

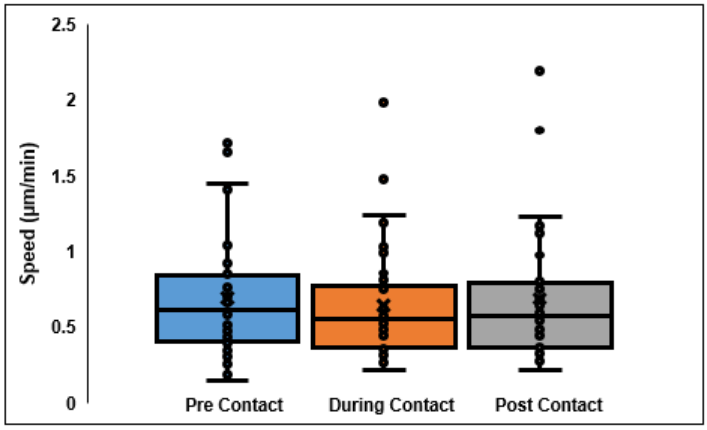

Figure 2.2. Average speeds for cell collisions pre contact, during contact and post contact. (n=18 collisions)

Next we observed that 29% of these head-head collisions resulted in one cell repolarizing, altering its migration direction and continued to migrate as a cohort with the other spindle (Figure 2.3a). We refer to this as non-mutual CIL as it does not follow the rules of traditional CIL where both cells are seen repolarizing post contact but rather only one cell out of the two will reverse its migration direction. In this scenario, we quantified the speeds of the both the spindle cell and the repolarizing spindle cell and compared them through pairing. We conclude that the spindle with a lower speed pre contact will be the one that ultimately repolarizes upon contact (Figure 2.3b, c).

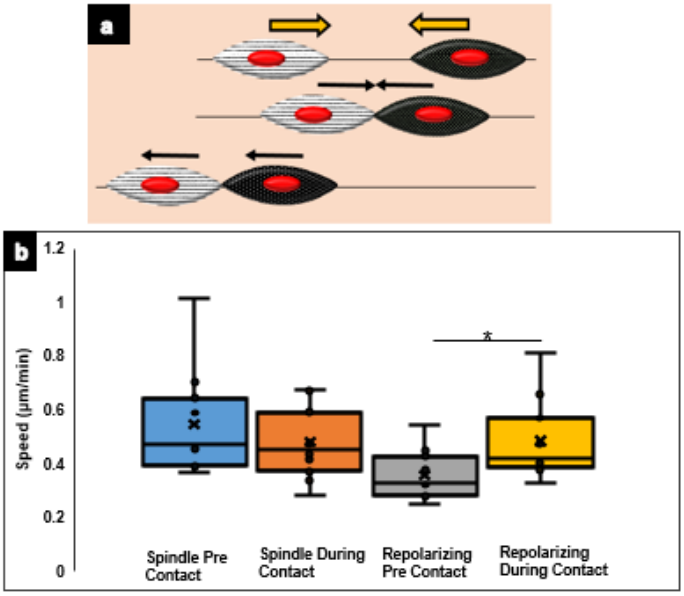

Figure 2.3. a) Representative sketch of two spindles approaching with one repolarizing and altering migration direction. **b)** Average speeds for cell collisions pre and during contact (n=11 collisions). (*, $p < 0.05$)

Lastly, a rare occurrence, occurring in only 4% of the collisions, two approaching spindles upon contact will both repolarize and form protrusions in the opposite direction of migration, described as the standard CIL observed on 2D substrates (Figure 2.4).

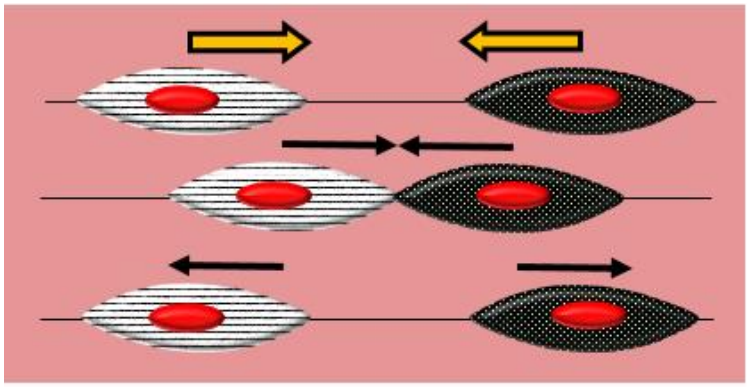

Figure 2.4. Representative sketch of traditional CIL rules of two approaching spindles, repolarizing, and altering their migration directions away from one another post contact.

2.2 Leading-Leading collisions with cell division

Mitotic daughter cells on flat 2D substrates are well known to separate and migrate away from each other at high speeds. In a similar fashion, we found spindle daughters to also move apart at significantly faster speeds (Figure 2.5). Through our CIL experiments, cell division was a prominent event that occurred when observing cell-cell collisions.

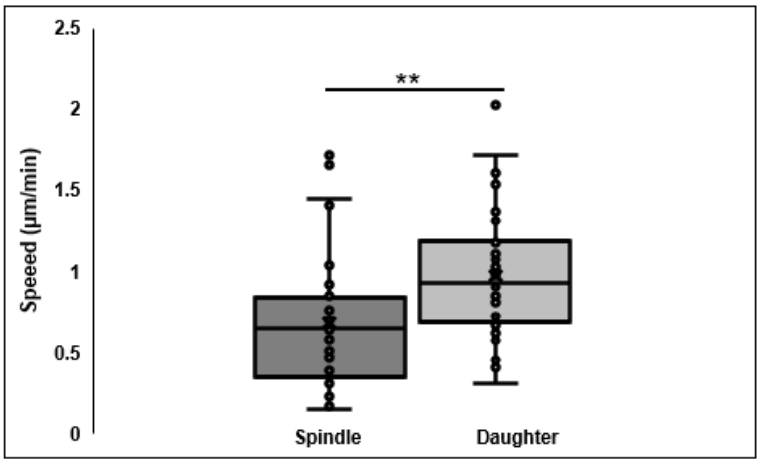

Figure 2.5. Plot comparing average cell speeds of a single spindle vs. daughter cell. (n=36 cells). (**, $p<0.01$)

Therefore, we wanted to see the mitotic division effect on the outcome of two approaching spindle cells and compare it to results of collisions without cell division. Similar to the outcome without division, although increased, 82% of approaching spindle cells came into contact, walked past one

another and continued to migrate in their respective directions without repolarization (Figure 2.6). This was concluded based from 98 randomly selections collisions.

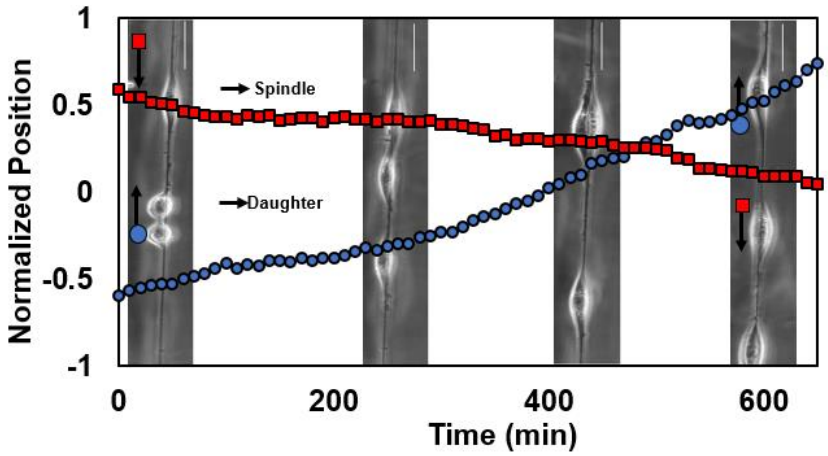

Figure 2.6. Transient profile of two approaching spindles, daughter (blue), spindle (red) walking past one another without repolarization. Scale bars: 50µm

We concluded that the daughter cell was significantly faster than that of a normal spindle pre contact. The speed for the daughter cell dropped during the contact period and the cell did not regain speed post contact (Figure 2.7).

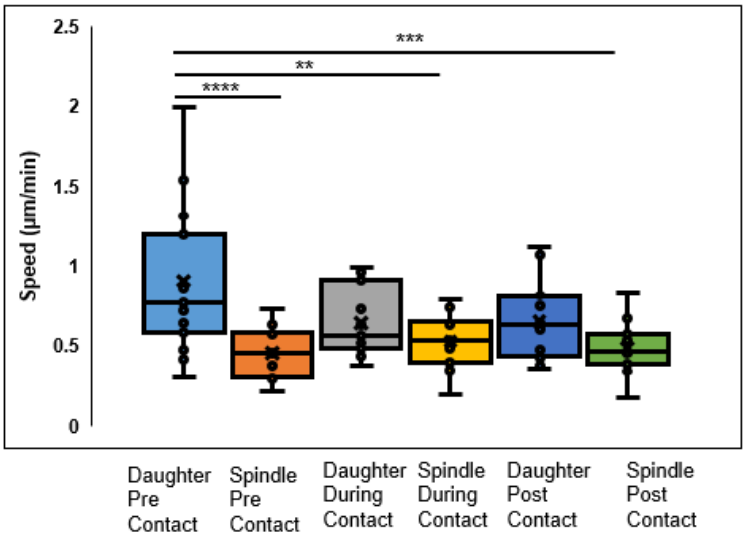

Figure 2.7. Average speeds of cell collisions for the daughter and spindle cell pre contact, during contact and post contact. (n=16 collisions) ((****, p<0.0001; ***, p<0.001; **, p<0.01)

In the presence of division, two approaching cells came into contact and 17% of the time, only one cell repolarized while they both proceeded to migrate as a unit similar to the behavior seen without division (Figure 2.8a). In this case, the non-daughter cell was not always the one to repolarize as in some instances, the daughter would repolarize and alter its migration direction instead (Figure 2.8b). We quantified the average speeds of the spindle and repolarizing spindle pre and during contact and represented the behavior through a paired data plot allowing comparisons between the speeds of the two cells (Figure 2.8c).

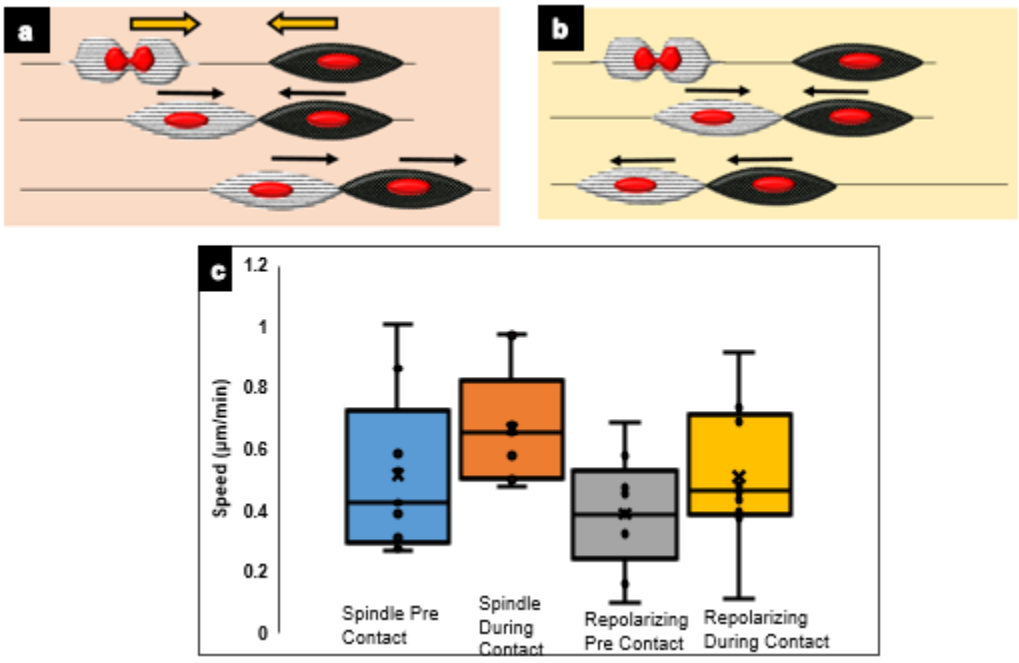

Figure 2.8. Representative sketch of two spindles approaching with the non-daughter **(a)** and daughter **(b)** repolarizing and altering migration direction**. c)** Average speeds for cell collisions pre contact, during contact (n=9 collisions).

To further compare the events for non-division and division CIL, we compared the time in contact prior to walk-past for both scenarios and concluded that with the occurrence of division,

the contact duration was shorter than that of cell collisions without division, although not significantly (Figure 2.9).

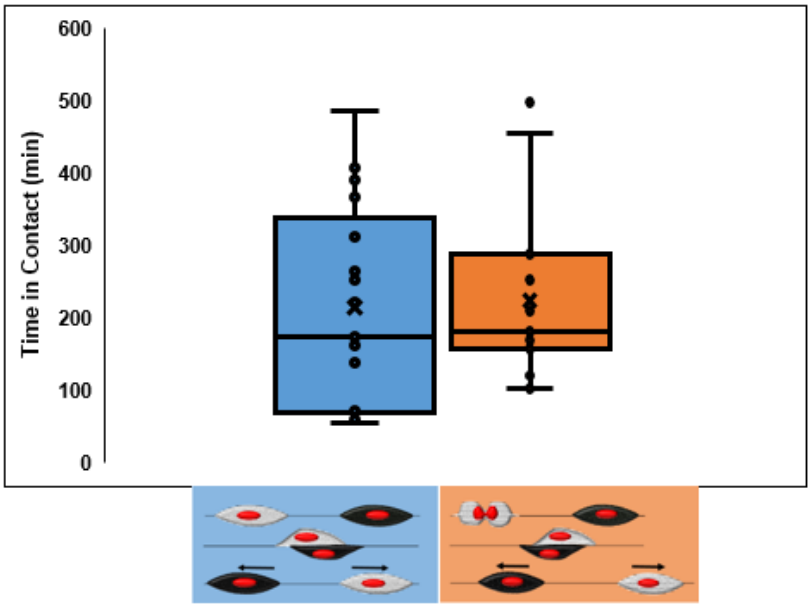

Figure 2.9. Comparison of time in contact for spindle leading-leading, walk-past collisions without and with division. (n=18,16 collisions)

Additionally, for the repolarization cases, we quantitated the time it took after contact for the repolarizing cell to extend its protrusions toward the opposite direction with and without the presence of cell division. As suspected, we observed that the repolarization time for a spindle with the incorporation of division was significantly faster than that without division (Figure 2.10).

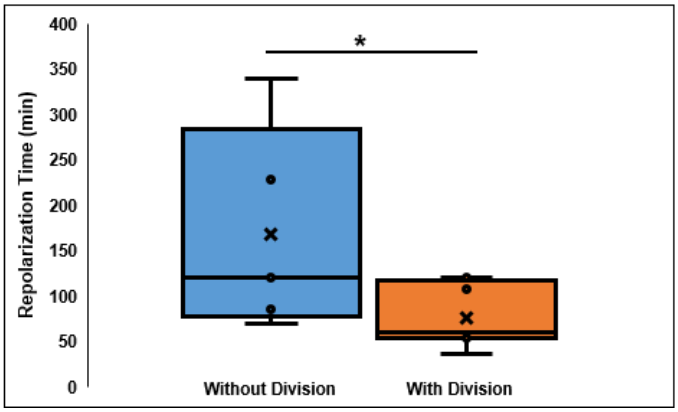

Figure 2.10. Comparison of time it takes to repolarize for spindle leading-leading, repolarization collisions without division and with division. (n=11, 9 collisions) (*, $p < 0.05$)

In conclusion, we report that the most prominent behavior in two approaching spindles on nanofibers, regardless of cell division, is that of a walk-by post contact without any repolarization occurring.

2.3 Leading-Trailing collisions

In addition to leading-leading or head-head collisions, we also observed instances where the leading edge of one spindle would contact the trailing edge of another spindle and both cells would continue to migrate as a unit. This has been seen in other CIL studies as well where authors term this behavior as contact following of locomotion (CFL) or head-tail cell collisions[14,28]. In CFL studies, it has been reported that a CIL response results in the repolarization of the trailing cell whereas the leading cell remains persistent[28]. Alternatively, here, a spindle termed trailing cell will contact a spindle in front of its path termed leading cell and will cause the leading cell to gain speed during contact (Figure 2.11a). We quantified the speeds pre and during contact and reveal that the trailing cell must be significantly faster than the leading cell in order to initiate contact and continue migrating (Figure 2.11b).

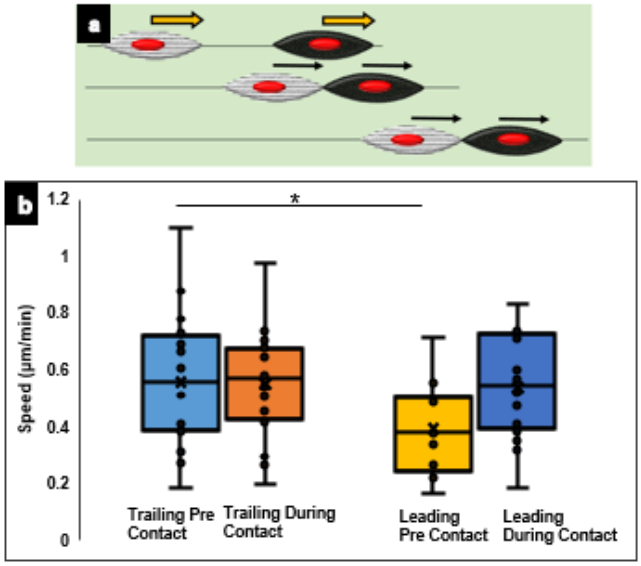

Figure 2.11. a) Schematic of leading-trailing collisions between spindle cells without division. **b)** Average speeds of trailing and leading cells pre and during contact (n=16 collisions). (*, $p < 0.05$)

The trend observed was similar for leading-trailing collisions in the presence of cell division as well Figure 2.12).

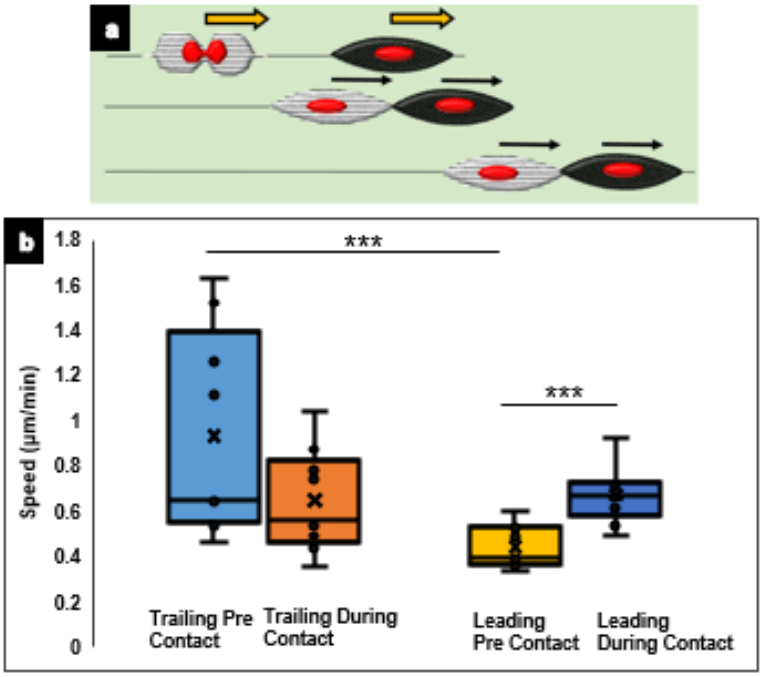

Figure 2.12. a) Schematic of leading-trailing collisions between spindle cells with division. **b)** Average speeds of trailing and leading cells pre and during contact. (n=9 collisions) (***, $p<0.001$)

Chapter 3. Parallel Cell CIL

3.1 Leading-Leading collisions without cell division

In addition to spindle cell CIL, we also qualitatively and quantitatively studied parallel cell CIL between two approaching cells. In cases where there was no cell-division, out of 26 collisions, we report that 100% of the time the cell pair will come into contact and result in one cell repolarizing (Figure 3.1).

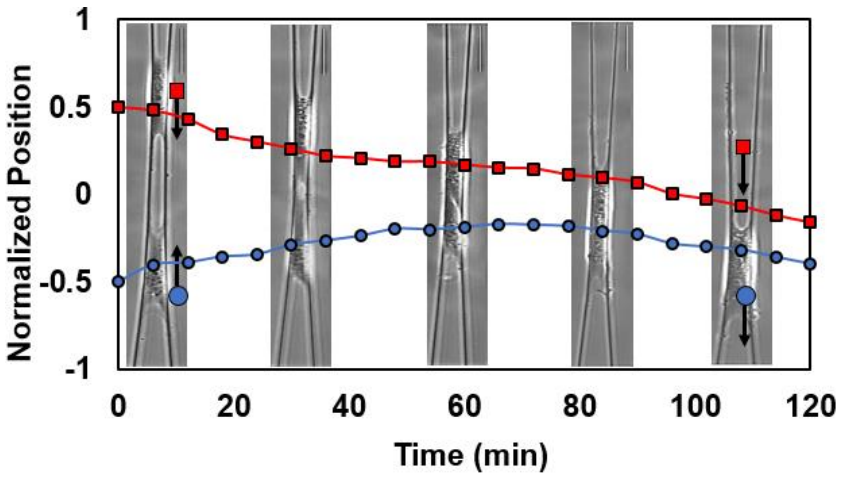

Figure 3.1. Transient profile of two approaching parallel cells, showing repolarization of one (blue arrow) upon contact. Scale bars: 50µm

We believe that this occurs due to fiber spacing constraint that induces a parallel shape. Unlike spindles, parallel cells do not have the ability to maneuver past and walk by one another as easily because they are adhered to two fibers instead of a single like spindle cells. Like the behavior reported in spindle cases, we term this non-mutual CIL as both the cells do not switch their migration direction. The speeds of both the parallel and repolarizing remain consistent pre and during contact without any significance which is consistent with our previous findings as no cell division is occurring (Figure 3.2).

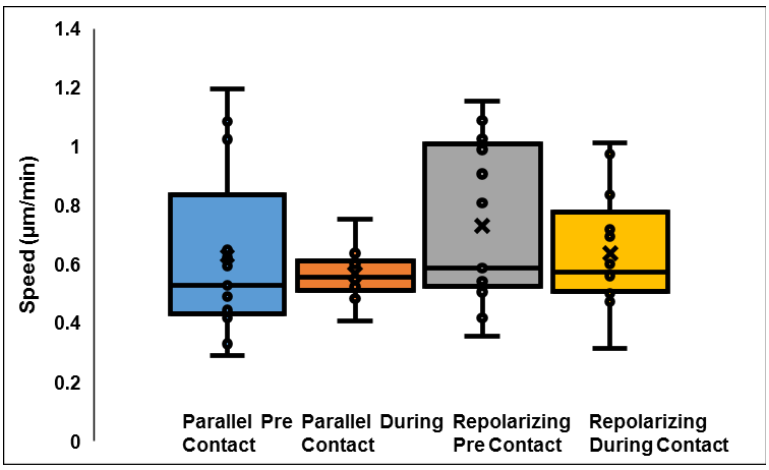

Figure 3.2. Average speeds for cell collisions pre and during contact for the parallel and repolarizing parallel during leading-leading collisions without division. (n=13 collisions).

3.2 Leading-Leading collisions with cell division

With the presence of cell division, out of 61 random collisions observed, we report that 62% of time the dividing cell will approach the non-dividing parallel cell and they will walk-by one another without repolarization (Figure 3.3). This behavior is similar to that of two approaching spindle cells as well. However, this walk-past is only possible if during the contact period, the parallel changes its shape to that of a spindle in order to surpass and then it regains its morphology post contact and continues to migrate.

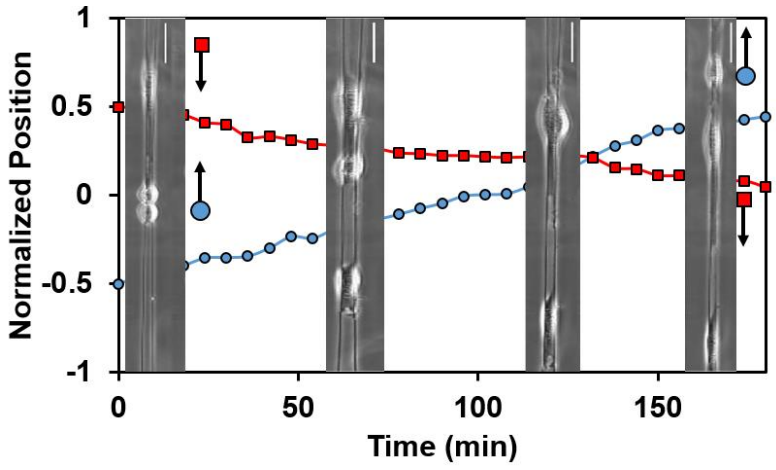

Figure 3.3. Transient profile of two approaching parallel cells, daughter (blue) non-daughter (red) walking by one another with the parallel cell changing morphology to that of a spindle cell during the contact period. Scale bars: 50µm

With respect to cell speeds, we report that the daughter cell loses speed during this contact period and further decreases in speed post-contact. Similarly, the non-dividing parallel also loses speed during the contact period and picks it up once it detaches from the daughter cell (Figure 3.4).

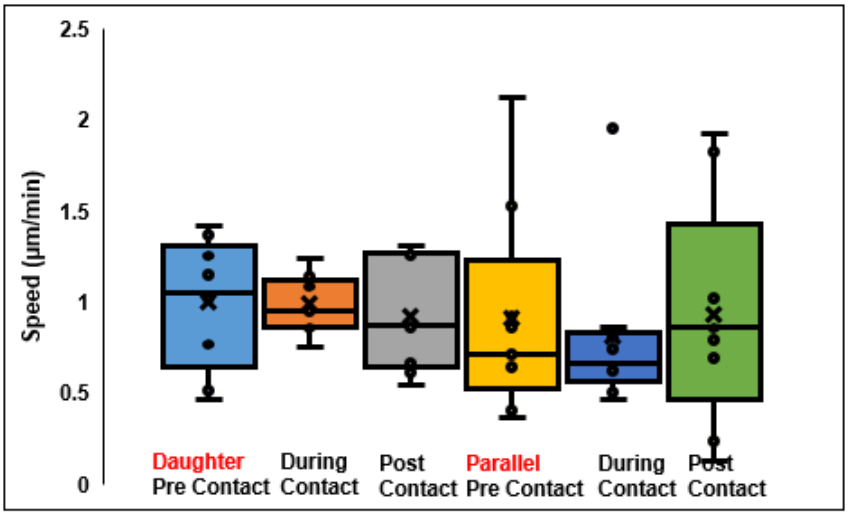

Figure 3.4. Average speeds for cell collisions pre, during and post contact for the daughter and parallel cells during walk-past. (n=9 collisions)

A rare (7 collisions/ 15%) yet extremely intriguing phenomenon seen in parallel cell CIL is that of a cell 'push'. In cell push cases, two parallel cells approached one another and prior to contact, one cell divided. The newly formed daughter cell initiated contact with the non-daughter and rapidly caused the non-daughter cell to repolarize and begin migrating in the opposite direction. In this scenario, one is able to visualize a "jamming plane" where both cells remained in contact and jammed against one another before cell repolarization took place **(**Figure 3.5**)** followed by the push behavior.

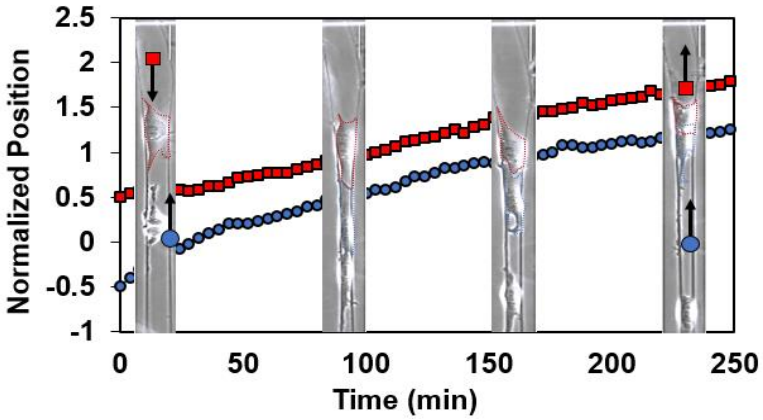

Figure 3.5. Transient profile of a cell push where the daughter cell (blue) post division, pushes the approaching parallel cell (red) causing it to repolarize toward the opposite direction (red arrow). Scale bar: 50µm

We believe that this is partly attributed to the significantly faster daughter cell speed post-division in comparison to that of a non-dividing parallel cell (Figure 3.6a). Furthermore, we report that the daughter cell during contact significantly loses speed as it is jamming with the subsequent cell (Figure 3.6b).

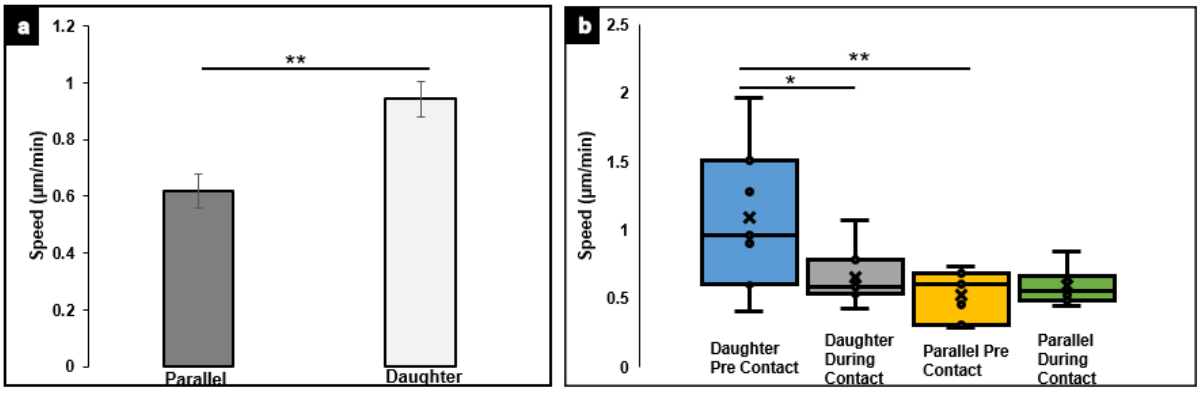

Figure 3.6. a) Plot displaying comparison between average speeds of parallel vs. daughter cell.(n=20) **b)** Graph revealing average speeds of daughter and parallel cell pre and during contact for cell push cases (n=7 collisions). (**, $p<0.01$; *, $p < 0.05$)

In a similar scenario, we report two parallel cells approaching, however as in this case, the cell jam followed by a push is not visible. For this behavior, we observe 23% of the time, a daughter cell post cell division approaches a parallel cell and the collision results in the parallel cell repolarizing, similar to a spindle CIL case described previously (Figure 3.7a). Here, we conclude that the

daughter cell significantly loses speed during contact with the approaching parallel cell whereas the parallel cell gains speed during the collision period (Figure 3.7b).

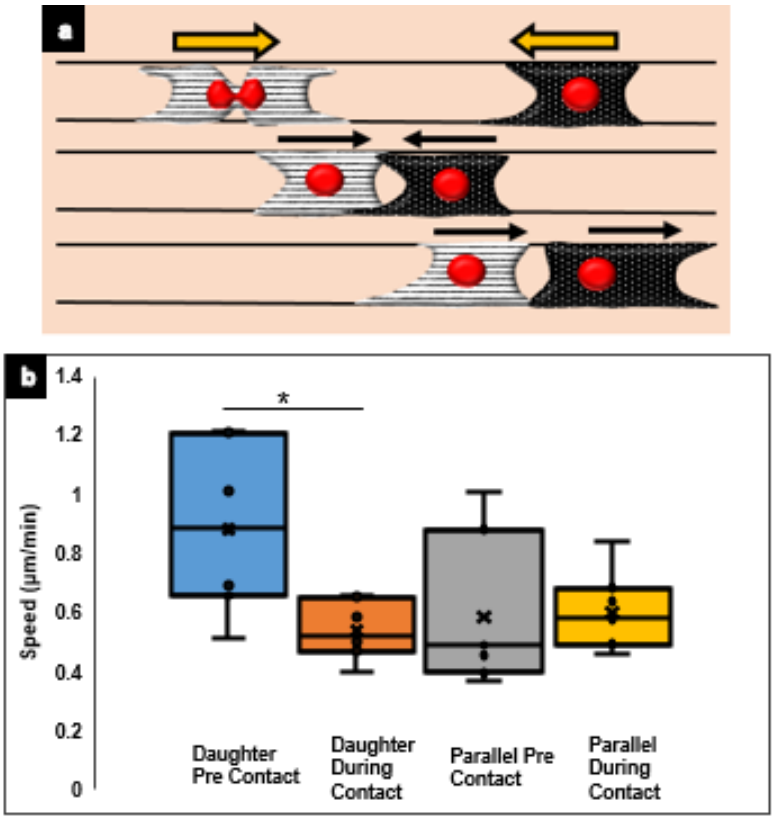

Figure 3.7. a) Schematic showing the leading-leading repolarization interaction between a daughter and parallel cell post cell division. **b)** Graph revealing average speeds of daughter and parallel cell pre and during contact (n=7) (*, $p < 0.05$)

In addition to cell speeds for non-division and division cases, we wanted to understand whether the starting distances between the cell centroids differed in order to define a criterion for cell push. We thus concluded that the starting distance between the centroids for two cells approaching without division involved was significantly larger than that leading to a cell push (Figure 3.8a). This allows us to infer that for a push to occur, the post division, the daughter cell immediately contacts the non-dividing parallel resulting in it being pushed and repolarized. Moreover, the

duration for repolarization for a non-division approaching case is longer than that seen when a cell push occurs, where the parallel repolarizes faster (Figure 3.8b).

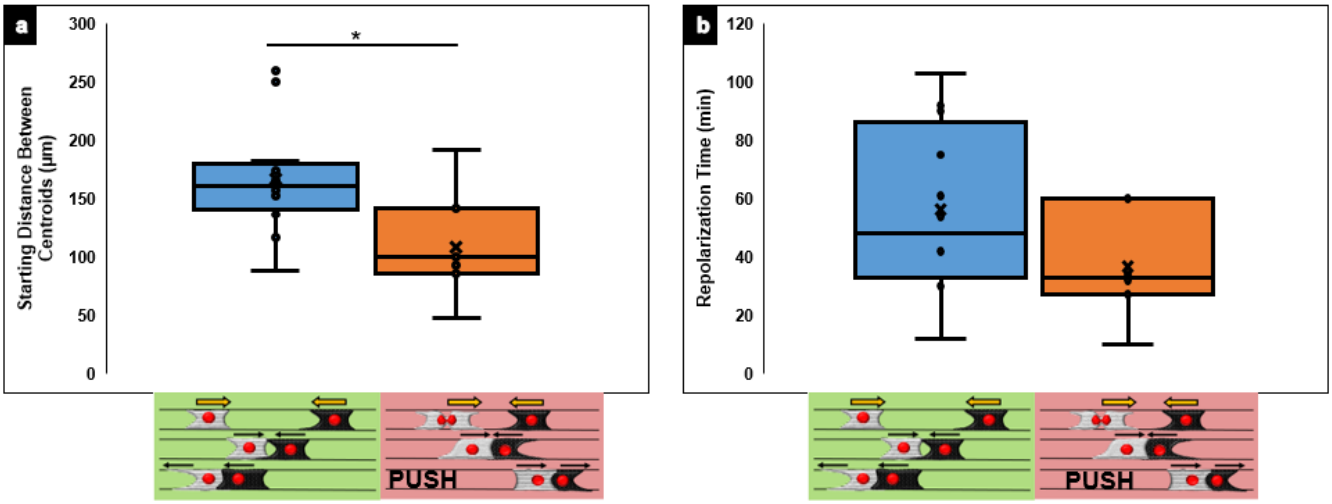

Figure 3.8. a) Plot comparing of starting distance between centroids of leading-leading, no division cases and cell push (n=13,7) **b)** Plot comparing time it takes for parallel cell to polarize for leading-leading and push cases(n=13,7) (*, $p < 0.05$)

3.3 Leading-Trailing collisions

Through our studies of parallel cell CIL, we also report the occurrence of leading-trailing (head-tail) collisions with and without cell division (Figure 3.9a). Once again, like spindle leading-trailing collisions, in parallel cells without cell division, we report that the trailing cell is significantly faster than the leading cell pre contact, which allows for it to make contact (Figure 3.9b).

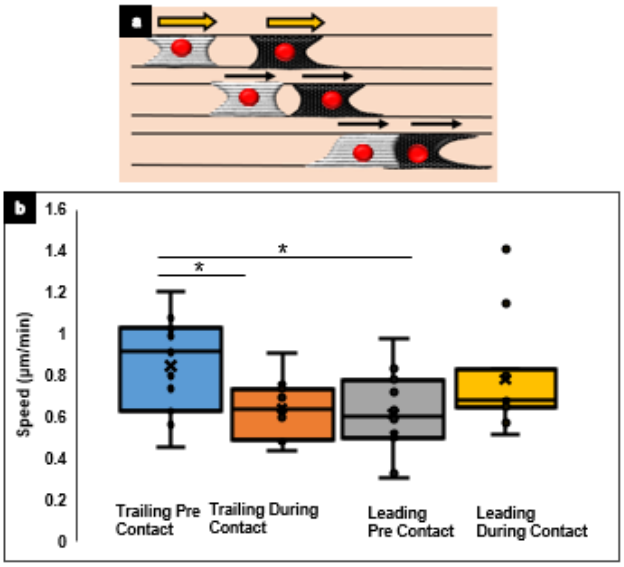

Figure 3.9 a) Schematic of leading-trailing collisions between parallel cells without division. **b)** Average speeds of trailing and leading cells pre and during contact. (n= 11 collisions) (*, $p < 0.05$)

During the contact duration, the leading cell gains speed and both cells continue to migrate as a cohort in the same direction. Likewise, with the occurrence of cell division, the trailing cell has a higher average speed before the contact period in order to reach the leading cell and induce its speed (Figure 3.10).

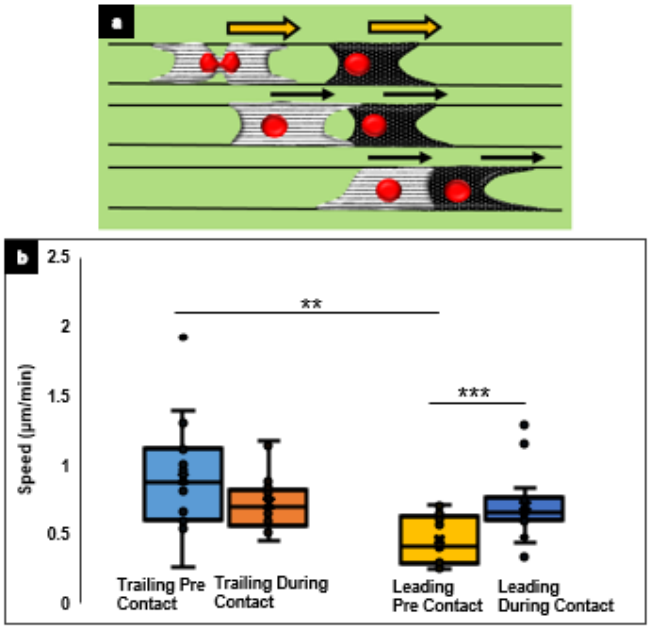

Figure 3.10 a) Schematic of leading-trailing collisions between parallel cells with division. **b)** Average speeds of trailing and leading cells pre and during contact. (n=17 collisions) ($p<0.0001$; ***, $p<0.001$; **, $p<0.01$)

Chapter 4. Spindle-Parallel CIL

4.1 Leading-Leading collisions without cell division

We also wanted to inquire about the outcome following an interaction between a spindle and parallel cell without the influence of cell division. Although the occurrence of such collisions is rare, we were able to identify certain patterns and rules for these interactions as well. When a parallel and spindle cell approach one another, the spindle will repolarize and continue migrating as a unit with the parallel cell. However, upon contact, the spindle both maintains its shape and proceeds with the migration or it alters its morphology to that of a parallel cell (Figure 4.1).

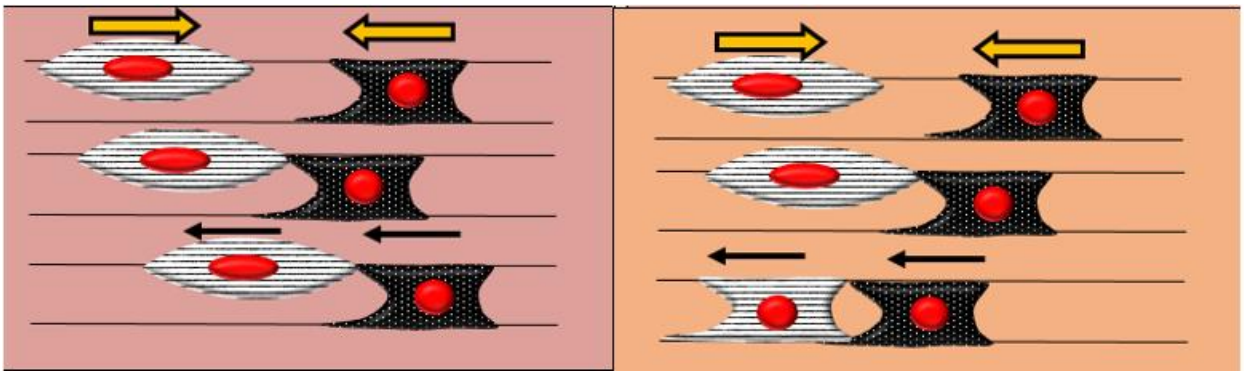

Figure 4.1. Schematic showing two different outcomes of spindle-parallel leading collisions.

We quantified speeds for both cells pre and during contact and show that both the spindle and parallel cells experience a slight decrease in speed during contact (Figure 4.2). However, we were only able to analyze 3 such collisions thus the sample size will need to increase for more conclusive results.

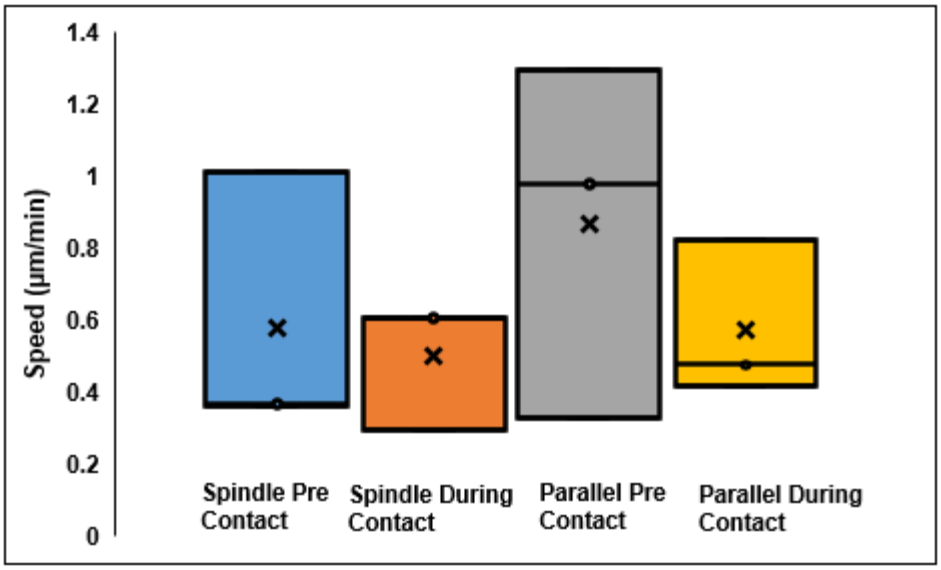

Figure 4.2. Plot depicting average speeds of spindle and parallel cells pre and during contact with one another. (n=3)

Another shared behavior among these cell-cell collisions was the walk-past. Similar to the walk-past described with two approaching parallel cells, in this scenario, the parallel cell has to alter its morphology to that of a spindle shape in order to walk-by and continue in its original migration direction (Figure 4.3).

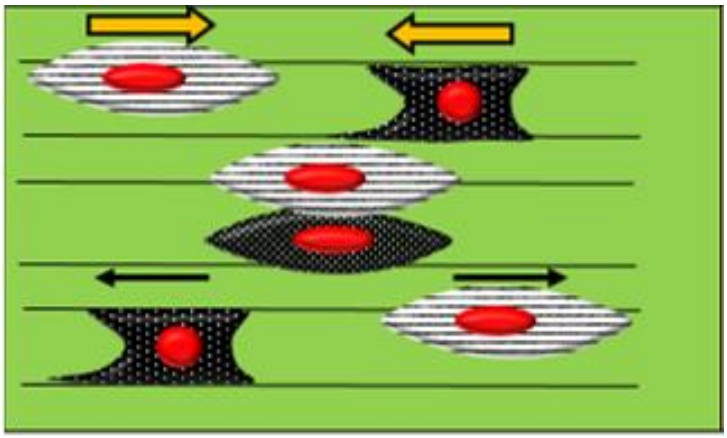

Figure 4.3 Schematic showing the outcome of spindle-parallel leading collisions with walk-past.

Out of 4 analyzed collisions, we see that the spindle cell loses speed during the contact period and regains speed post contact with the parallel cell. Similarly, the parallel cell also experiences

a decrease in speed during contact but unlike the spindle cell, it further loses speed during the post contact period (Figure 4.4).

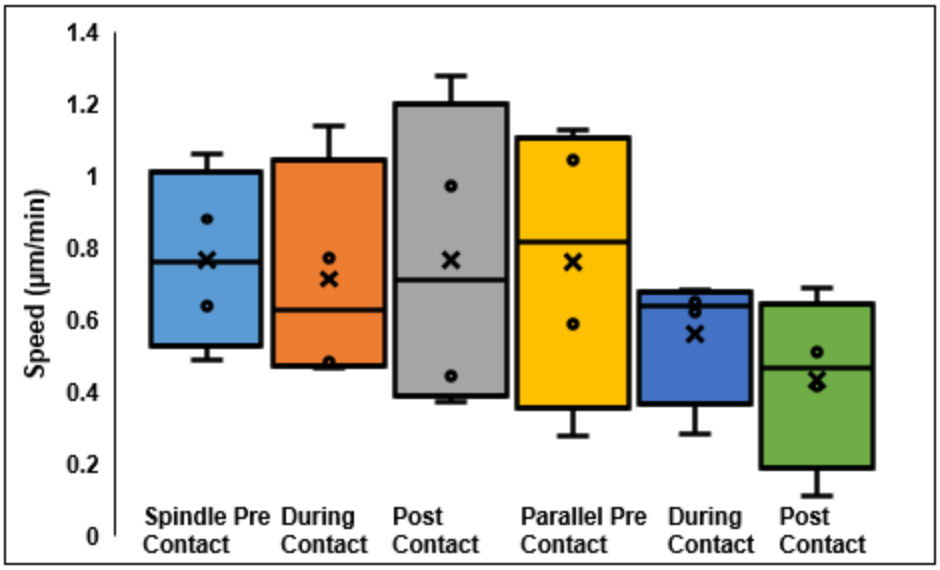

Figure 4.4. Plot depicting average speeds of spindle and parallel cells pre, during and post contact with one another. (n=4)

Once again, we report these speeds based off of 4 cell collisions and aim to increase this sample size with more experimentation.

4.2 Leading-Leading collisions with cell division

Spindle-parallel cell collisions also occur post mitotic cell division. When approaching, the spindle cell divides, repolarizes and alters its shape to that of a parallel cell before continuing to migrate as a cohesive with the parallel cell. However, in this case, the spindle is not always the one to divide. We report parallel cell division as well which results in contact with the spindle leading to its repolarization and new migration direction either maintaining its spindle shape or altering it to that of a parallel (Figure 4.5).

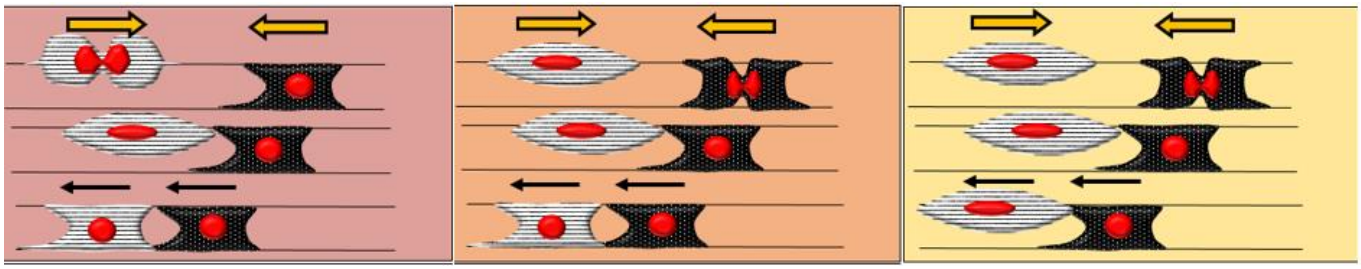

Figure 4.5 Schematic showing the varying outcome of spindle-parallel leading collisions with division and repolarization.

We analyzed 6 such collisions and quantified their speeds distinguishing between the spindle and the parallel (Figure 4.6a) or comparing them based off the daughter vs. non-daughter cell (Figure 4.6b). We show that the spindle and parallel cell lose speed during the contact period as do the daughter and non-daughter cell.

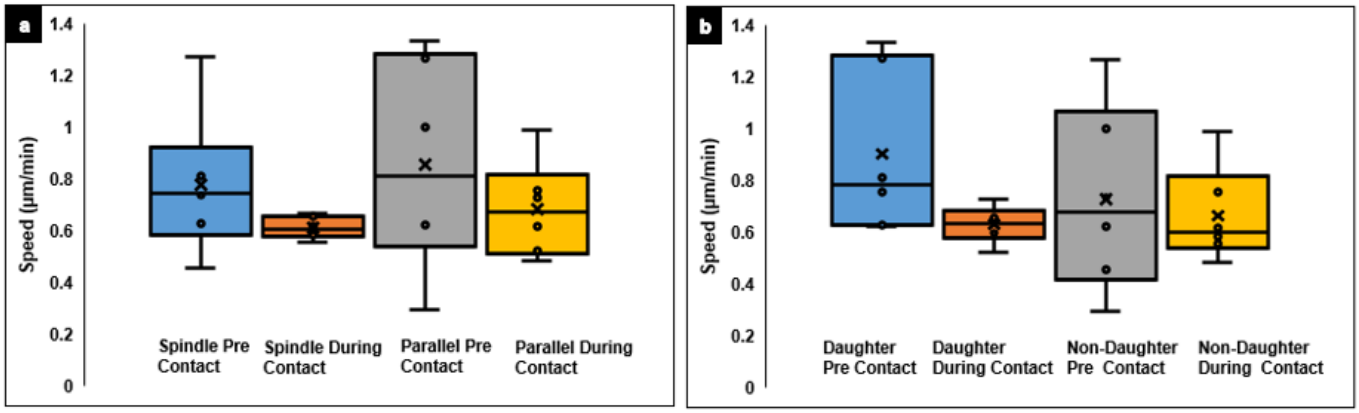

Figure 4.6. **a)** Plot depicting average speeds of spindle and parallel cells pre and during contact with one another. **b)** Plot comparing average speeds of daughter vs. non-daughter cell pre and during contact. (n=6 collisions)

Next, we looked at the walk-past behavior with the effect of cell division and report similar behavior. We reveal that in this case, the spindle or parallel can identify as the daughter cell and regardless, the parallel cell must change its shape to a spindle during the contact period in order to walk-past the spindle and continue in its original migration direction (Figure 4.7).

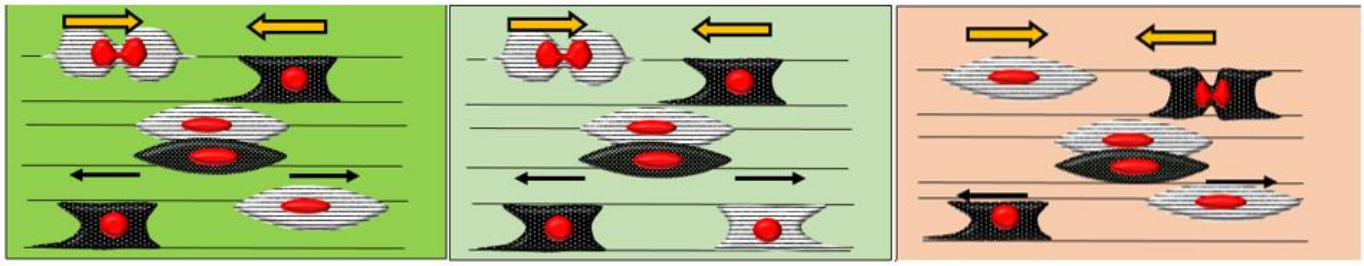

Figure 4.7. Schematic showing the varying outcome of spindle-parallel leading collisions with division and walk-past.

Once again, we quantified the speeds by comparing the spindle to the parallel cell or the daughter to the non-daughter based off 4 collisions. The spindle cell loses speed during contact and regains it post contact with the parallel cell. Contrastingly, the parallel cell gains speeds during the contact period, where it takes the form of a spindle and drops back to its original speed during the post contact period (Figure 4.8a). When looking at the daughter vs non-daughter cell speeds, we report similar patterns. The speed of the daughter cell decreases during the contact period and remains consistent post contact as well. Alternatively, the non-daughter picks up speed during the contact period and experiences a slight decrease post-contact (Figure 4.8b).

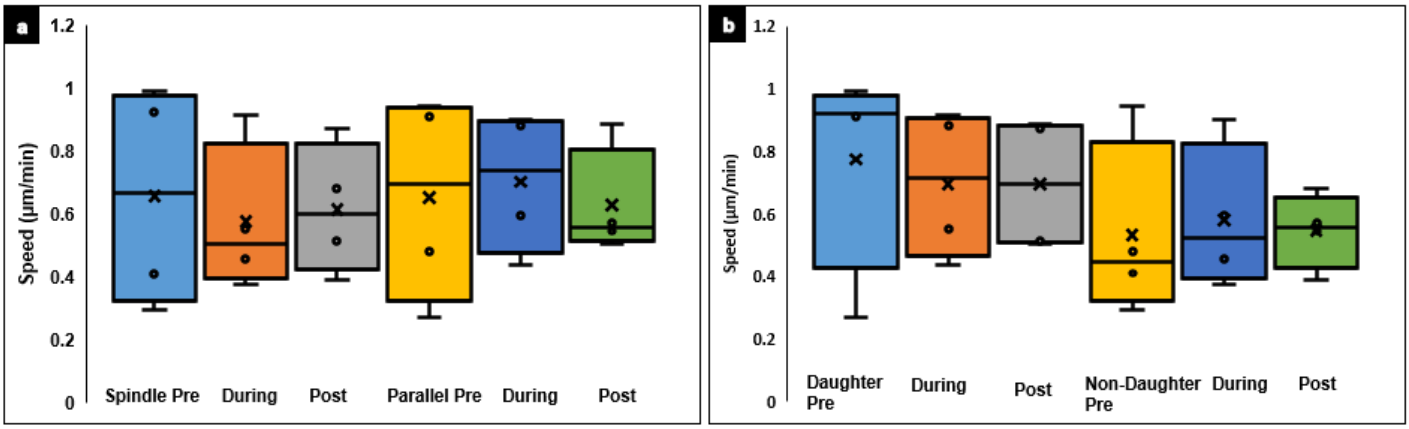

Figure 4.8. **a)** Plot depicting average speeds of spindle and parallel cells pre, during and post contact with one another. **b)** Plot comparing average speeds of daughter vs. non-daughter cell pre and during contact. (n=4 collisions)

4.3 Leading-Trailing collisions

Leading-trailing collisions between a spindle and parallel cell also occur with and without cell division. When a spindle and parallel are migrating in the same direction without cell division, we observe that either cell can identify as the leading or trailing. Similar to previous leading-trailing scenarios, we reveal that the trailing cell must be faster than the leading cell in order to initiate contact and continue migration. A spindle cell once again either maintains its original shape during contact or alters it to that of a parallel during and post the migration period (Figure 4.9).

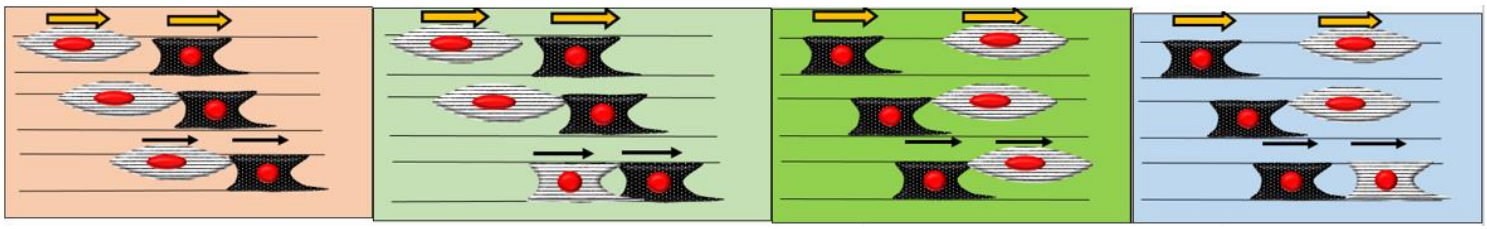

Figure 4.9. Schematic showing the varying outcome of spindle-parallel leading collisions without division for leading-trailing collisions.

With the influence of cell division, we report four varying rules for spindle-parallel collisions (Figure 4.10). Firstly, when the spindle divides, the daughter cell (trailing cell) will contact the leading parallel cell and either remain a spindle or become a parallel cell before migrating as a unit with the cell. Similarly, when a parallel cell divides, the trailing daughter will contact the leading spindle which will maintain or change its morphology during the contact period.

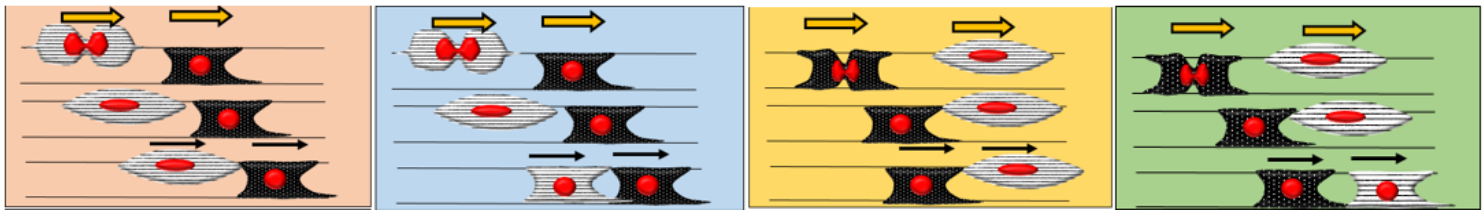

Figure 4.10. Schematic showing the varying outcome of spindle-parallel leading collisions with division for leading-trailing collisions.

Once again, we report that the trailing cell must be significantly faster than the leading cell in order to catch up and create contact. Furthermore, we reveal that the leading cell gains speed following contact with the trailing cell during these collisions (Figure 4.11).

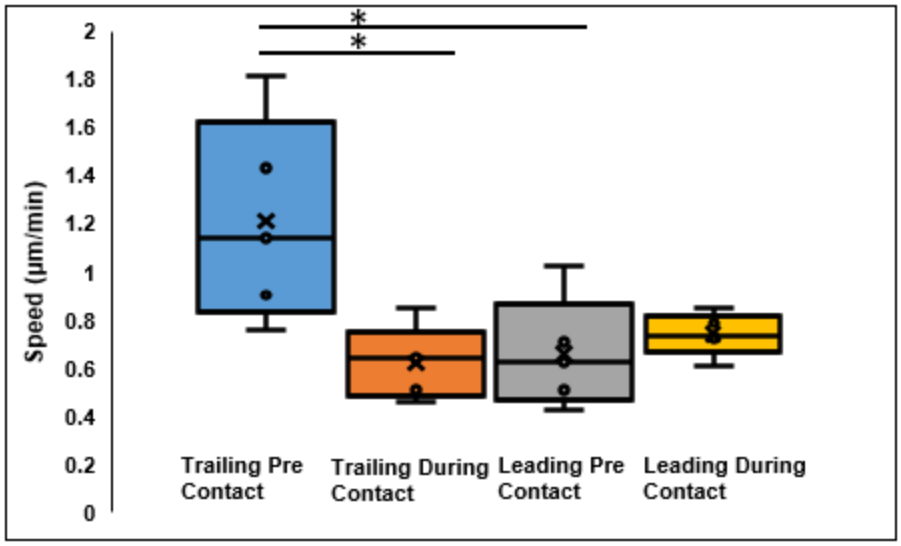

Figure 4.11. Plot depicting average speeds of leading (spindle or parallel) and trailing (spindle or parallel) cells pre and during contact. (n=5 collisions) (*, $p < 0.05$)

We were able to quantify 5 such leading trailing collisions and only 2 such leading-trailing collisions without division. Thus, we aim to expand upon the sample size in the future to solidify our results.

Chapter 5. Geometric Rules in multi-cell interactions

Next, we did not want to limit our studies to strictly observing and quantitating CIL between only two cells. Although, the two cell CIL provided us a basis for understanding cell migratory patterns upon contact, we wanted to expand our experimental approach and attempt to understand what takes place when multiple cells encounter one another. When observing multi-cell CIL, cells became fairly confluent overtime, completely populating the fibers. We hypothesized that this would result in a loss of CIL as cells do not have the ability or space to maneuver past or avoid one another thus having relevance to physiological processes such as cancer metastasis. This was further supported by cells beginning to form spheroid- like structures, where they migrated into a single unit. Overtime, these cells began to slowly trickle out of this spheroid morphology and restart the contact inhibition of locomotion process in a cyclic manner (Figure 5).

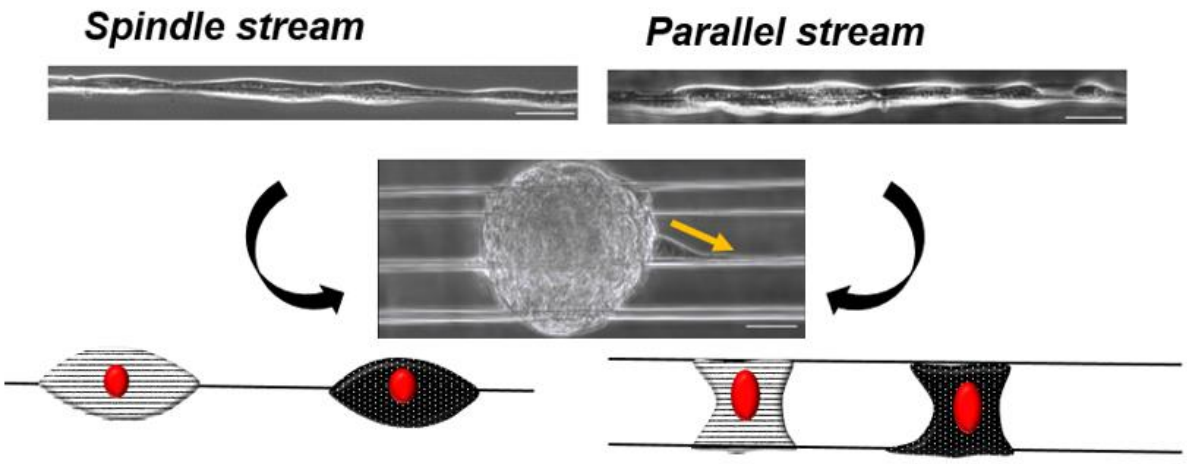

Figure 5.1. Schematic showing multi-cell interactions leading to spheroid formation overtime. Single cells begin emerging from spheroid and are subjected to two cell collision CIL rules representing a cyclic CIL process. Scale bars: 50µm

Chapter 6. Discussions and Conclusions

Contact inhibition of locomotion (CIL) occurs when two cells upon contact, alter their protrusive behavior, repolarize and begin to migrate in a new direction, away from the site of contact. The relevance of CIL has been linked to biological processes such as wound healing[11] and its loss to cell cancer cell invasion and metastasis[9]. A cell's native extracellular matrix (ECM) is fibrous in nature and the alignment of these fibers has been associated with metastasis promotion. Therefore, it would be beneficial to study how cells maintain their traditional CIL rules in an environment that mimics *in vivo* like properties. Here, we present, for the first time, a platform to quantitate CIL geometrical rules in 3T3 fibroblast cells of diverse morphologies resembling *in vivo* shapes. Using suspended fibers in aligned patterns, we investigate CIL decisions of two cells approaching each other in two elongated shapes: spindle cells attached to single fibers, and parallel cells attached to two fibers in a 1D manner. Similarly, 1D collision assays with micropatterned, fibronectin lines have been previously utilized as a strategic technique to study CIL[26]. Advantages to this approach include, cell control and confinement to the lines which induces the collision occurrence among cells. These approaches differ from previous methods to analyze CIL which include 2D invasion assays[8] that require labeling explants and analyzing cell angles to quantify behavior.

Interestingly, with our platform, we observe two approaching spindle cells upon contact, do not repolarize but rather pass by one another and continue along their respective migration direction. This behavior is similar to a "walk-past" used to describe cells on micropatterned lines where they also pass by one another without repolarization[26]. Notably, this walk-past behavior was the least probable to occur among their identified CIL scenarios whereas in our case, spindle-spindle crossover occurs most frequently. Previously, a walk past behavior on 2D substrates was extracted based off an overlap index[38]. This index value was obtained by estimating the number of cell nuclei

that are expected to overlap upon a random distribution of cells compared to the actual number of overlaps. Therefore, the ratio of observed to expected was the value reported. In 2D studies, Abercrombie and colleagues observed that a walk past between approaching cells mostly occurred upon a leading edge of the underlapping cell passing by under the side of overlapping cell[38]. With respect to cell speed, they also observed a reduction in speed upon collision with another cell[10]. Contrastingly, when two parallel cells approach one another, upon contact, one cell will repolarize, switch its migration direction and continue to move as a unit with the other. These behaviors differ from the traditional CIL definition as both cells do not inhibit their protrusive behavior and alter their migration path as seen in initial studies[11]. However, it has been previously acknowledged that the sequence of CIL events can be altered due to cell response thus resulting in the redirection of just one cell[1]. Furthermore, we concluded for a spindle and parallel cell to crossover one another without alteration in their respective migration directions, the parallel cell will have to conform to the morphology of a spindle during the cell-cell contact period in order to continue its migration as it does not have the ability to do so with its present physical shape.

Additionally, we were able to determine that cell division has significant influences on both spindle and parallel CIL. Both spindle and parallel daughter cells post division migrate at a significantly faster speed than that of a non-daughter cell. Although this did not affect the outcome of spindle cell CIL for two approaching cells in terms of migration trajectories, it did impact two trailing spindles, originally moving in the same direction. In this scenario, the leading cell upon contact with the trailing cell will experience an increase in speed. Similarly, two trailing parallel cells experience the same effect upon contact with one another. This behavior can be attributed to the speed of the daughter cell post division, where upon contact the trailing cell will also be affected, resulting in an increase in its speed. Therefore, this leading-trailing response is only possible if the

trailing cell is faster than the leading pre contact. In previous CFL studies, an increase in leading cell speed upon contact has not been reported. One rare but intriguing phenomenon we observe in parallel cell CIL is that of a cell "push." Here, two parallel cells approach one another, and one cell will undergo division. Following division, the daughter and parallel cell will contact, jam with one another, before the parallel cell repolarizes and is pushed in the opposite direction. The concept of cell jamming incorporates various factors such as cellular crowding, force transmission, cell adhesion and contractility[13]. We conclude that all cases of cell push require jamming whereas cell jamming itself does not necessarily result in a push.

Parameters we use to quantify CIL include cell speed, time in contact and the distance between cell centroids used to track cell migration. The normalized position over time allows one to follow the trajectory of the two cells, with the intersection point corresponding to the overlap of the cell centroids in spindle-spindle and spindle-parallel interactions. This is similar to analysis with cells plated on micropatterned lines[26] where authors used the distance between cell nuclei to track CIL. This allows for confined cell migration leading to a greater probabilistic outcome of CIL along with simplistic measurements. Also with regard to speed values for cell pairs during CIL, studies on micropatterned lines show that CIL occurs with similar frequency and duration for both 2D and 1D studies[26]. Also, the cellular protrusions and in terms of inhibition and reversal are comparable on both platforms. The cell speed trends reported in these studies are analogous to results in our experiments in terms of speed decreasing the during contact period with differences in actual values attributed to the variation in cell types used for studies. Additionally, speed values reported in the initial CIL studies from Abercrombie fell with the range of 0.3-0.6μm, for chick heart fibroblast cells, which are similar to our reported values[9].

Ultimately, we reveal the different outcomes of cell-cell collisions in sequential geometric rules for spindle and parallel shapes and identify the probabilistic outcome of each scenario. Spindle and parallel cell CIL differ in that crossover is most common in two spindle shaped cells as they can maneuver past one another due to cell shape and adhesion sites. However, parallel cell morphology restricts cells from intersecting unless cell division is involved. Furthermore, we observe the formation of cell streams post CIL wherein spindle and parallel cells will populate the fibers, resulting in limited cell movement due to confinement. The reduction in speed due to increased cell density has also previously been reported in context of contact inhibition, thus supporting our observations[39]. These cell streams conform into multi-cell, spheroid aggregates spanning multiple fibers. Eventually, the fibroblasts begin to escape from the spheroid resulting in a cyclic process wherein CIL will begin again.

In conclusion, we present, for the first time, a platform to quantitate CIL geometrical rules in cells of diverse morphologies (spindle and parallel) resembling *in vivo* shapes. Based upon these rules, we sequentially detail CIL decision steps in multiple cells attached to and migrating on the same fibers. We observe that an increasing number of cells causes cell clustering at localized positions in spheroidal aggregates. In the future, we would like to incorporate heterotypic CIL studies with our STEP platform to understand if and how these defined geometric rules are altered.

Chapter 7. Future Directions

7.1 Effect of fiber diameter on CIL outcomes

We would like to extend our CIL studies by incorporating outcomes of cell collisions with alternations in fiber diameter. Previously, we discussed conducting experiments on 500nm fibers due to the advantages in protrusion visibility and quantification of speed pre, during and post contact. This was concluded after preliminary studies with 130nm fibers where we observed plasticity in cell shape and longer protrusions, where cell migration was not easily predictable. Whereas, with the 1000nm fibers, the protrusions of each cell were harder to discern due to the larger diameter. We observed single cell collisions on both these alternative diameters (Figure 6.1) and hypothesize that on the smaller, 130 nm diameter, the walk past behavior would significantly decrease if not completely be eliminated due to the long protrusions making their inhibition

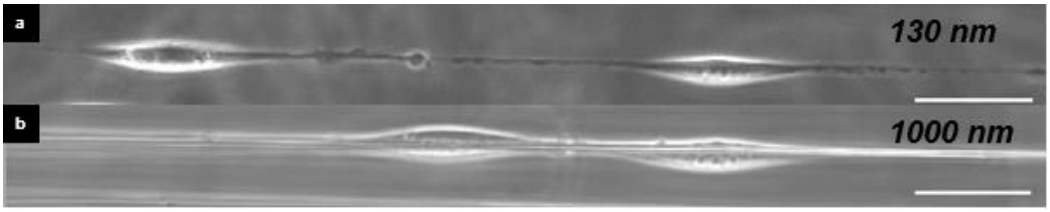

Figure 7.1. a) Single spindle cell interactions on 130 nm depicting longer cellular protrusions. **b)** Two interacting spindle cells on 1000nm fiber. Scale bars: 50µm.

difficult for cells and thereby further complicating their migratory path past/over one another. With respect to the 1000nm fibers, we conclude the visibility of the cell protrusions decreases and further infer that the increase of adhesion strength would not allow the cells to walk past one another.

7.2 Influence of biological inhibitors on CIL behavior

Previous CIL studies have shown the effect of biological inhibitors on CIL outcomes. As discussed, RhoGTPases have a strong influence in controlling the molecular machinery of cells and more specifically the repulsion response during CIL. Predominantly, it has been concluded that inhibition of the protein ROCK, via Y27632 stabilizes a cells microtubules, resulting in a loss of CIL[7,26]. Additionally, authors reported that a co-treatment with nocodazole, rescues this CIL response why allowing microtubules to conform to their dynamic nature with shrinkage and growth[7]. We conducted preliminary studies with three different concentrations of the ROCK inhibitor, Y27632, a small (5µM), medium (10µM) and large (30µM) based off the values reported in literature. We began by quantitating single cell speeds for both parallel and spindle shaped cells on 500nm PS fibers (Figure 6.2). We concluded that there was no significant difference between cell speeds, although for the parallel cell we did observe a direct relationship between the speed and inhibitor concentration.

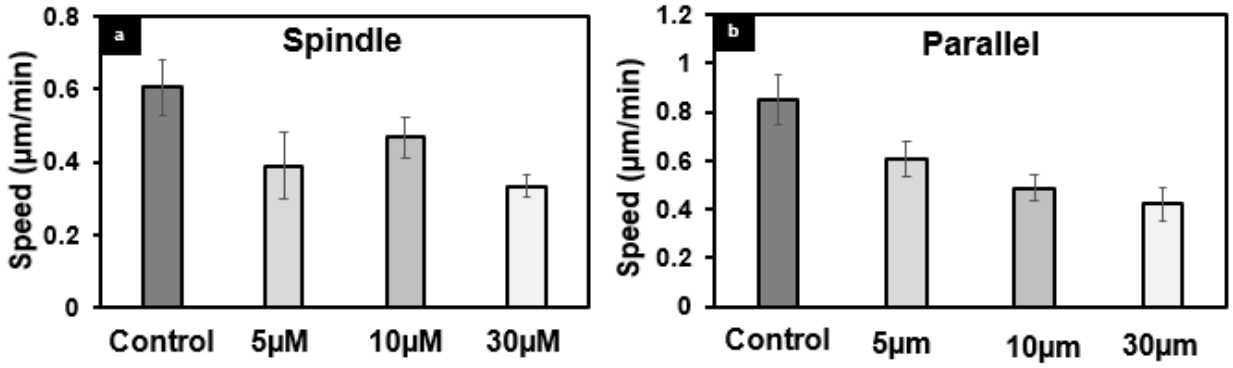

Figure 7.2. a) Single spindle cell speed for three different concentration of Y27632. **b)** Single parallel cell speed for three Y27632 concentrations. n.s, n=10 cells per category.

We would like to extend these studies to qualitatively and quantitatively define CIL behavior for two cells approaching (head-head) and trailing (head-tail) collisions and conclude whether inhibiting ROCK activity diminishes the CIL response on nanofibers as well.

7.3 Heterotypic CIL

Throughout our experimentation, we primarily focused on homotypic CIL interactions between two fibroblast cells and determined their outcomes post collision. However, heterotypic CIL has been reported to hold a significance in cancer cell metastasis. In cell populations such as sarcoma cells (connective tissue cancer cells) and fibroblast, its been observed that there is a loss of heterotypic CIL, resulting in the ability of the cancerous cells to invade the fibroblast population[19,40]. However, this does not necessarily imply that homotypic interactions between cancer cells also lead to a loss of CIL, as such homotypic interactions follow the traditional CIL response of repulsion and redirection. Additionally, while neural crest cells, a migratory embryonic cell population, maintain homotypic CIL among themselves, they are reported to lose a heterotypic CIL response allowing them to invade the mesoderm layer and other tissues[1]. Therefore, we would like to expand our current studies to also determine heterotypic CIL outcomes both on a flat, 2D platform as well as the STEP platform with nanofibers (Figure 6.3).

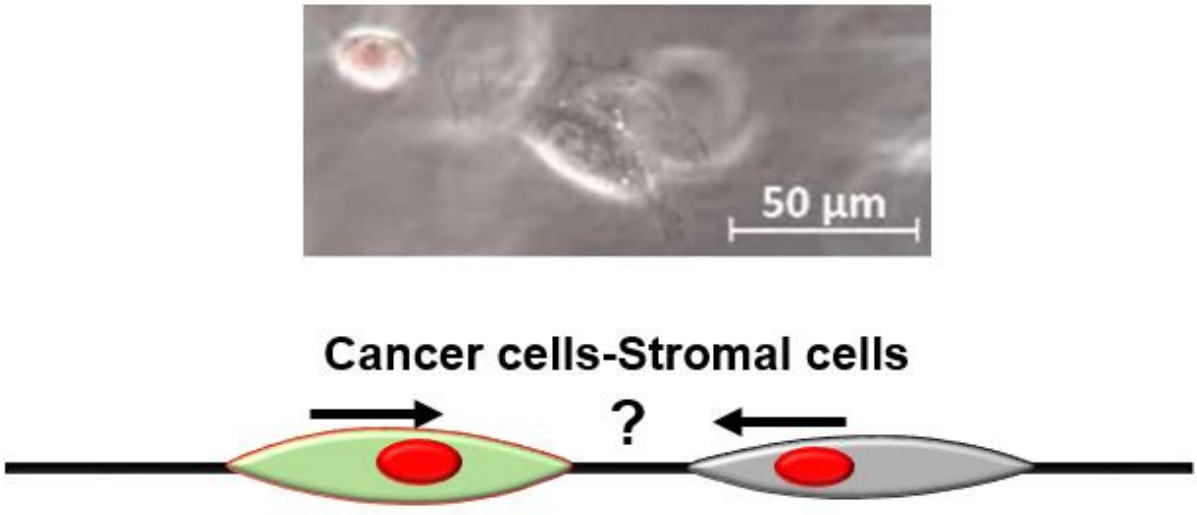

Figure 7.3 CIL between a pancreatic cancer cell and 3T3 fibroblast on a flat, 2D substrate (top image). Extension of heterotypic CIL between cancer and stromal cells on nanofibers with unknown outcome upon collision (bottom image).

Our studies introduce a new platform that mimics a cell's natural fibrous environment through the generation of nanofibers to study CIL behavior. Thus, these studies incorporate an additional model to address fundamental questions in the field of cell biology with respect to physiological and developmental processes that are impacted by CIL.

References

1. Mayor, R. & Carmona-Fontaine, C. Keeping in touch with contact inhibition of locomotion. *Trends Cell Biol.* **20**, 319–328 (2010).

2. Rozario, T. & DeSimone, D. W. The extracellular matrix in development and morphogenesis: A dynamic view. *Dev. Biol.* **341**, 126–140 (2010).

3. Rosso, F., Giordano, A., Barbarisi, M. & Barbarisi, A. From Cell-ECM Interactions to Tissue Engineering. *J. Cell. Physiol.* **199**, 174–180 (2004).

4. Campetelli, A., Bonazzi, D. & Minc, N. Electrochemical regulation of cell polarity and the cytoskeleton. *Cytoskeleton* **69**, 601–612 (2012).

5. Schmidt, S. & Friedl, P. Interstitial cell migration: Integrin-dependent and alternative adhesion mechanisms. *Cell Tissue Res.* **339**, 83–92 (2010).

6. Ridley, A. J. *et al.* Cell Migration: Integrating Signals from Front to Back. *Science (80-.).* **302**, 1704–1709 (2003).

7. Kadir, S., Astin, J. W., Tahtamouni, L., Martin, P. & Nobes, C. D. Microtubule remodelling is required for the front-rear polarity switch during contact inhibition of locomotion. *J. Cell Sci.* **124**, 2642–2653 (2011).

8. Carmona-fontaine, C. *et al.* Contact inhibition of locomotion in vivo controls neural crest directional migration. **456**, 957–961 (2008).

9. Abercrombie, M. & Heaysman, J. E. Observations on the social behaviour of cells in tissue culture. II. Monolayering of fibroblasts. *Exp. Cell Res.* **6**, 293–306 (1954).

10. Abercrombie, M. & Heaysman, E. M. OBSERVATIONS ON THE SOCIAL BEHAVIOUR.

11. Abercrombie, M. Contact inhibition and malignancy. *Nature* **281**, 259–262 (1979).

12. Friedl, P., Locker, J., Sahai, E. & Segall, J. E. Classifying collective cancer cell invasion. *Nat. Cell Biol.* **14**, 777–783 (2012).

13. Sadati, M., Taheri Qazvini, N., Krishnan, R., Park, C. Y. & Fredberg, J. J. Collective migration and cell jamming. *Differentiation* **86**, 121–125 (2013).

14. Li, D. & Wang, Y. L. Coordination of cell migration mediated by sitedependent cell-cell contact. *Proc. Natl. Acad. Sci. U. S. A.* **115**, 10678–10683 (2018).

15. © 1954 Nature Publishing Group. (1954).

16. Abercrombie, A. & Ambrose, A. J. The Surface Properties of Cancer Cells : A Review. (1962).

17. Carmona-Fontaine, C., Matthews, H. & Mayor, R. Directional cell migration in vivo: Wnt at the crest. *Cell Adh. Migr.* **2**, 240–242 (2008).

18. Davis, J. R. *et al.* Inter-cellular forces orchestrate contact inhibition of locomotion. *Cell* **161**, 361–373 (2015).

19. Stramer, B. & Mayor, R. Mechanisms and in vivo functions of contact inhibition of locomotion. *Nat. Rev. Mol. Cell Biol.* **18**, 43–55 (2017).

20. Kay, J. N., Chu, M. W. & Sanes, J. R. MEGF10 and MEGF11 mediate homotypic interactions required for mosaic spacing of retinal neurons. *Nature* **483**, 465–469 (2012).

21. Theveneau, E. *et al.* Collective Chemotaxis Requires Contact-Dependent Cell Polarity. *Dev. Cell* **19**, 39–53 (2010).

22. Oldfield, F. E. Orientation behavior of chick leucocytes in tissue culture and their interactions with fibroblasts. *Exp. Cell Res.* **30**, 125–138 (1963).

23. Martinez-Rico, C., Pincet, F., Thiery, J. P. & Dufour, S. Integrins stimulate E-cadherin-mediated intercellular adhesion by regulating Src-kinase activation and actomyosin contractility. *J. Cell Sci.* **123**, 712–722 (2010).

24. Lin, B., Yin, T., Wu, Y. I., Inoue, T. & Levchenko, A. Interplay between chemotaxis and contact inhibition of locomotion determines exploratory cell migration. *Nat. Commun.* **6**, (2015).

25. Theveneau, E. *et al.* Chase-and-run between adjacent cell populations promotes directional collective migration. *Nat. Cell Biol.* **15**, 763–772 (2013).

26. Scarpa, E. *et al.* A novel method to study contact inhibition of locomotion using micropatterned substrates. (2013). doi:10.1242/bio.20135504

27. Davis, J. R. *et al.* Emergence of embryonic pattern through contact inhibition of locomotion. *Development* **139**, 4555–60 (2012).

28. Desai, R. A., Gopal, S. B., Chen, S. & Chen, C. S. Contact inhibition of locomotion probabilities drive solitary versus collective cell migration. *J. R. Soc. Interface* **10**, 20130717 (2013).

29. Kulawiak, D. A., Camley, B. A. & Rappel, W. J. Modeling Contact Inhibition of Locomotion of Colliding Cells Migrating on Micropatterned Substrates. *PLoS Comput.*

Biol. **12**, (2016).

30. Wang, J. & Nain, A. S. Suspended micro/nanofiber hierarchical biological scaffolds fabricated using non-electrospinning STEP technique. *Langmuir* **30**, 13641–13649 (2014).

31. Nain, A. S. *et al.* Tissue engineering. 1153–1159 (2008). doi:10.1002/smll.200800101

32. Nain, A. S., Sitti, M., Jacobson, A., Kowalewski, T. & Amon, C. Dry spinning based spinneret based tunable engineered parameters (STEP) technique for controlled and aligned deposition of polymeric nanofibers. *Macromol. Rapid Commun.* **30**, 1406–1412 (2009).

33. Jana, A. *et al.* Crosshatch nanofiber networks of tunable interfiber spacing induce plasticity in cell migration and cytoskeletal response. *FASEB J.* fj.201900131R (2019). doi:10.1096/fj.201900131r

34. Sheets, K., Wunsch, S., Ng, C. & Nain, A. S. Shape-dependent cell migration and focal adhesion organization on suspended and aligned nanofiber scaffolds. *Acta Biomater.* **9**, 7169–7177 (2013).

35. Doyle, A. D., Wang, F. W., Matsumoto, K. & Yamada, K. M. One-dimensional topography underlies three-dimensional fi brillar cell migration. *J. Cell Biol.* **184**, 481–490 (2009).

36. Harley, B. A. C. *et al.* Microarchitecture of three-dimensional scaffolds influences cell migration behavior via junction interactions. *Biophys. J.* **95**, 4013–4024 (2008).

37. Friedl, P. & Wolf, K. Plasticity of cell migration: A multiscale tuning model. *J. Cell Biol.* **188**, 11–19 (2010).

38. Heaysman, J. E. M. Contact Inhibition of Locomotion: A Reappraisal. *Int. Rev. Cytol.* **55**, 49–66 (1978).

39. Schnyder, S. K., Molina, J. J., Tanaka, Y. & Yamamoto, R. Collective motion of cells crawling on a substrate: Roles of cell shape and contact inhibition. *Sci. Rep.* **7**, 1–14 (2017).

40. Abercrombie, M. & Heaysman, J. E. M. Observations on the social behaviour of cells in tissue culture: I. Speed of movement of chick heart fibroblasts in relation to their mutual contacts. *Exp. Cell Res.* **5**, 111–131 (1953).

Appendix:

Appendix A: Speed box and whisker plot description

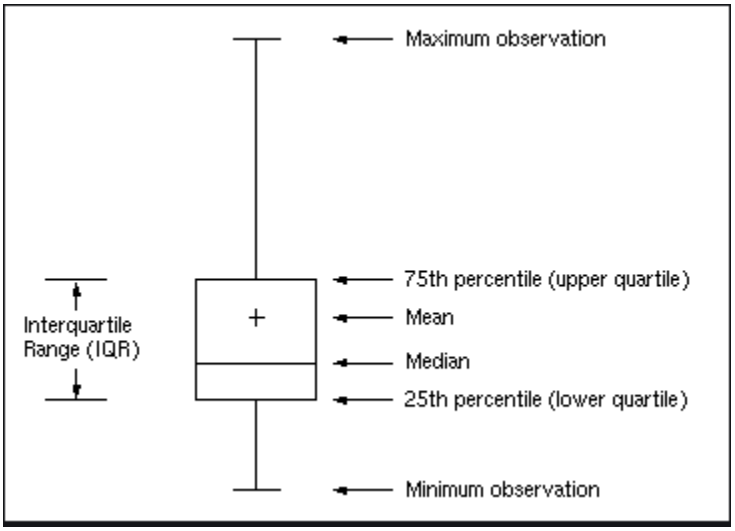

Image credit: Support.sas.com

Appendix B: Transient profile generation reference